Energy Conversion and Management 292 (2023) 117326

Contents lists available at ScienceDirect

Energy Conversion and Management

journal homepage: www.elsevier.com/locate/enconman

A mixed integer linear programming-based simple method for optimizing the design and operation of space heating and domestic hot water hybrid systems in residential buildings

E. Pérez-Iribarren [a,*], I. González-Pino [a], Z. Azkorra-Larrinaga [a], M. Odriozola-Maritorena [b], I. Gómez-Arriarán [b]

[a] ENEDI Research Group, Department of Energy Engineering, Faculty of Engineering of Bilbao, University of the Basque Country UPV/EHU, Plaza Torres Quevedo 1, Bilbao 48013, Spain

[b] ENEDI Research Group, Department of Energy Engineering, Faculty of Engineering of Gipuzkoa, University of the Basque Country UPV/EHU, Europa Plaza 1, 20018 Donostia, Spain

ARTICLE INFO

Keywords:
Thermal systems
Hybridization
Linear programming
Multicriteria optimization
Energy efficiency in buildings

ABSTRACT

The hybridization of energy systems is based on the combined integration of both renewable and non-renewable technologies and thermal energy storage. These hybrid installations improve cost effectiveness and energy efficiency when they are correctly designed and the operation strategy is suitable. Despite the relevance of achieving the optimal configuration, sizing and control strategy of hybrid thermal systems, there is no simple and generic methodology which allows this type of installations to be optimized in the project phase. In response to this issue, in this work, a mixed integer linear programming-based simple model is carried out with the aim of obtaining the optimal design, sizing and operation of thermal energy systems in residential buildings. To do so, a superstructure is defined that includes the main technologies commercialized for thermal energy systems in buildings. Technical, economic, environmental and legal constraints are determined in the proposed generic model. In order to validate the method, it is applied to a central space heating and domestic hot water installation of a residential building located in a cold climate in Spain. Optimal solutions are obtained considering three different perspectives —economic, environmental and multicriteria— and are compared to the current installation. According to the results, the overall cost of the economic optimal configuration is reduced by 15%, whereas the greenhouse gas emissions decrease by 56% in the environmental optimal solution. It is thus demonstrated that the proposed generic and simple model is a useful tool for determining the optimal hybridization of the plant and for analysing the technical, economic and environmental feasibility of these systems in the project phase.

1. Introduction

In 2018, households accounted for about 26.1% of the final energy consumption in the European Union [1], the greenhouse gas (GHG) emissions associated with this sector being 776 million tons of carbon dioxide equivalent ($CO_{2\text{-eq}}$) —19% of the total GHG emissions [2]. The current energy situation leads engineers to thoroughly consider which technologies or energy sources suitable for the residential sector are better for the end-users. A flexible coupling of renewable and non-renewable technologies with thermal energy storage (TES) can contribute to reducing both the economic cost and the environmental impact, as well as to increasing the overall efficiency of the plant and the primary energy savings [3]. Nowadays, however, there is no simple and generic methodology for determining which technology within the commercially available systems is the most feasible–from an economic or environmental point of view- for a specific building.

There are different studies focused on analysing the challenges for the hybridization of energy systems, in which systems are modelled and then a simulation or an optimization is carried out. When simulation is

Abbreviations: BB, biomass boiler; CB, condensing boiler; CTE, Technical Building Code; CHP, Combined Heat and Power; DHW, domestic hot water; GHG, greenhouse gas; HP, heat pump; HT, high temperature; ICE, Internal Combustion Engine; LTB, low temperature boiler; LHV, Low Heating Value; LT, low temperature; MILP, Mixed Integer Linear Programming; MINLP, Mixed Integer Non-Linear Programming; PV, photovoltaic; ST, solar thermal; TES, Thermal Energy Storage.

* Corresponding author.
E-mail address: estibaliz.perezi@ehu.eus (E. Pérez-Iribarren).

https://doi.org/10.1016/j.enconman.2023.117326
Received 27 December 2022; Received in revised form 10 June 2023; Accepted 19 June 2023
Available online 5 July 2023

Nomenclature

B	binary variable for boilers
bin	binary
BIN	binary variable
c	unit cost (€/kWh)
C	cost (€)
co_2	unit GHG emissions (kg of $CO_{2\text{-eq}}$/kWh)
CO_2	GHG emissions (kg of $CO_{2\text{-eq}}$)
COP	coefficient of performance (per unit)
CRF	capital recovery factor (-)
cw	specific heat of water (kJ/(kg·K))
d	day
E	electric energy (kWh)
$\dot{E}$	electric power (kW)
f	function
F	fuel energy (kWh)
$\dot{F}$	fuel power (kW)
FAM	environmental amortization factor (y^{-1})
fo	operation factor
G	global incident radiation (kWh)
h	hour (h)
HEAT	binary variable for space heating
HP	heat pump binary variable
i	annual interest rate (%)
ICE	internal combustion engine binary variable
Inv	total investment (€)
Lim	limit
M	constant of big M method
Min	minimize
n	lifetime (year)
ntd	number of times that each day is repeated (day/month)
PCT	percentage (%)
PES	primary energy saving (%)
PL	partial load (per unit)
PUR	binary variable for purchased electricity
Q	thermal energy (kWh)
$\dot{Q}$	thermal power (kW)
r	ratio
R	radiation
RC	renewable contribution
REE	equivalent electric efficiency (%)
$RefE_\eta$	harmonised efficiency reference value for separate production of electricity (%)
$RefH_\eta$	harmonised efficiency reference value for separate production of heat (%)
S	surface (m^2)
SOLD	binary variable for sold electricity
ST	solar thermal binary variable
t	period of time (h)
T	temperature (°C)
V	volume (l)
x	variable
Y	sizing variable

Greek symbols

ε	epsilon
η	efficiency (%)
ρ	density (kg/m^3)
λ	binary auxiliary variable
σ	orientation and inclination losses (%)

Subscripts

abs	absorbed
amb	ambient
ave	average
B	boiler
BB	biomass boiler
CB	condensing boiler
CAP	capacity of thermal storage
CHAR	charging process
DEM	demand
DHW	domestic hot water demand
DISCH	discharging process
DISS	dissipated energy
E	electricity
EPUR	purchased electricity
ESOLD	sold electricity
FM	fix maintenance
HEAT	heating demand
HP	heat pump
HT	high temperature
ICE	internal combustion engine
INV	investment
k	technology
LOSS	losses
LT	low temperature
LTB	low temperature boiler
MIN	minimum
NOM	nominal value
O&M	operation and maintenance
PUR	purchased
PV	photovoltaic
Q	heat
r	return
SOLD	sold
ST	solar thermal
STO	stored thermal energy
TES	thermal energy storage
TOT	total
U	useful
VM	variable maintenance
V-S	volume-surface

applied, the operation strategy of the integrated technologies is evaluated in order to analyse the economic feasibility [4] and the inefficiencies of the plant [5]. Regarding the optimization, heuristics methods —such as Genetic Algorithms, Tabu Search or Ant Colony— or mathematical programming —Mixed Integer Linear Programming (MILP) and Mixed Integer Non-Linear Programming (MINLP)— are used.

In the case of the heuristic methods, these have some advantages when compared with MILP, such as being very flexible, more efficient for large-size problems and being able to use non-linear constraints in models closer to the real functioning [6]. On the contrary, the achieved optimal solution cannot be the global optimum —since the algorithm can get trapped in a local optimum of the solution space, and the calculation method is dependent on the initial problem and its structure—, which have to be previously defined. Related to this last point, all the levels of optimization (operation, sizing and design) cannot be integrated and optimized together. Hence, these methods are used considering the operation optimization as a routine within an iterative optimization model of sizing, for installations whose design and configuration are previously defined [7].

Unlike heuristic models, MILP provides a global optimal solution and the possibility of solving large scale problems by means of a "horizontal algorithm", where the variables of operation, design and synthesis are treated in a similar way and at the same level. Thus, MILP models allow a comprehensive optimization of hybrid systems, from operation to design and synthesis. The principal barriers found to applying MILP models are related to the high mathematical complexity in their formulation and the linearization of non-linear problems, as well as the high computational time required in mid- and large-scale applications, where multiple decision variables and constraints are needed in order to model the behaviour of the plant. For these reasons, commercial solvers are usually used —which are sometimes expensive and have their own source code—, making it harder for their use to spread among engineers and researchers.

The MILP method is usually applied for determining the optimal energy distribution in smart-grids [8]. Some studies extend this analysis to multi-energy systems, where heating, cooling and electricity generation systems are considered. In [9], a MILP-based model was proposed for optimizing the control strategy of an urban area. In this case, the design of the generation systems was previously defined and the optimal strategy was compared to the conventional operation to determine the savings achieved with the proposed model.

The optimization of thermal systems usually has a uni-objective perspective, either minimizing the overall cost or maximizing the environmental benefits and energy savings. In [10], Samsatli presented a MILP model for simultaneously optimizing the design and operation of urban energy systems from an economic point of view. The size of the devices was previously defined and the optimization allowed the selection of conversion, storage and transport technologies and the operation of an eco-town network to be defined. Wang et al. proposed a MILP-based optimization model for minimizing the overall cost of cascade heat utilization in a district-scale microgrid [11]. This approach considered temperature grade differentiation and energy degrade utilization. It was therefore a more realistic and efficient model and increased the efficiency of distributed energy systems. Lozano et al. applied MILP to optimize the design of trigeneration systems installed in the tertiary sector [12]. A superstructure was defined to do so, where different energy supply systems were considered. In the optimal configuration, the amount of previously sized devices to be installed was optimized according to an economic perspective.

The most interesting configuration should provide greater energy savings, while ensuring service availability, generating the least possible environmental impact and being the most profitable technology. Nevertheless, there is no technology that can fulfil all these requirements at the same time; environmentally friendly technologies tend to have higher investment costs; whereas conventional technologies —with lower investment costs— have a greater environmental impact. Hence, applications in the residential sector require a methodology that enables the integration of thermal generation systems to be analysed in order to meet these objectives. In these cases, a multi-objective perspective should be applied to determine the solution spectrum which fulfils the different objectives, such as economic (cost minimization), thermodynamic (efficiency maximization) and environmental (environmental impact minimization).

Somma et al. [13] defined a multi-objective optimization model for optimizing the operation of an existing distributed energy system. They developed a multi-objective linear programming model to minimize the weighted sum of operation costs and environmental impact. It was concluded that the optimal operation can change considerably with the weight assigned to each objective. This study was later extended by the authors and applied to the multi-objective optimal sizing and operation of a hypothetic cluster of 30 buildings through cost and exergy assessments [14]. Apart from this, the influence of exergy on the sustainable development of energy supply systems was also analysed. Linear programming was also used in [15], where a multi-objective optimization of district heating systems was carried out. The principal aim of this work was to analyse the replacement of some devices —used for thermal energy supply— in a district heating network, considering the minimization of the total cost, the carbon dioxide emissions and the exergy destruction. Mavrotas et al. [16] provided a multi-objective optimization framework for energy planning by using the ε-constraint technique, which was applied to a hospital. Fazlollahi et al. [17] compared three multicriteria optimization methods for complex energy systems; whereas Alarcón-Rodríguez et al. [18] presented a review of the state-of-the-art of multi-objective planning of distributed generation technologies.

As mentioned above, MILP is mostly applied to distributed energy systems. Regarding residential applications, its use is not widespread. In [19], a MILP problem was defined for optimizing energy supply systems in buildings, which allowed equipment —whose size was previously defined— to be selected and the optimal operation to be determined. In this model, different technologies were considered for providing both thermal and electric energy to a domestic building. This work was extended in [20], where the envelope design was included. In the same vein, Schütz et al. implemented a MILP model for optimizing energy conversion units and envelopes of residential buildings [21]. The sizing of different technologies had been previously defined and the installed capacity was selected according to a multi-objective optimization.

Despite the fact that different MILP models have been carried out for planning district heating systems, few studies dealing with the optimal configuration of tertiary and residential sectors can be found in the bibliography. Apart from this, in these studies, the capacity and devices considered for each technology are previously determined, thus, not optimizing the sizing of the devices but only the selection of technologies or devices and operation of the plant, which has a great influence on the final results. It should be noted that these models are rarely validated and compared with real solutions. Finally, another disadvantage is that these models are usually implemented by means of commercial solvers, due to the numerous variables and constraints of the problem, which reduces the possibility of spreading its use for real applications.

As a contribution to this discussion, a simple and easily reproducible MILP-based model is proposed in this article in order to determine the technical, economic and environmental feasibility and optimize the configuration, sizing and operation of hybrid thermal systems in residential buildings. Nowadays, the configuration and sizing of thermal installations are traditionally determined by means of rough methods, which result in oversized equipment and a reduced overall efficiency of the plant. The information obtained by this method is essential in the project phase, where the optimal technologies have to be selected and sized, considering not only the design of hybrid thermal systems, but also their combined operation. Unlike other MILP models, the technologies are not pre-sized, so their capacity is optimized along with the configuration and the overall operation of the plant. Apart from this, the problem herein presented is applied to a real, recently constructed building, thus allowing the model to be validated by comparing the results achieved to those measured in the real plant. Furthermore, the model is implemented in an Open Source solver, whose code is efficient, available, simple and easy to use, which considerably enhances its dissemination. Since the real behaviour of thermal plants obeys non-linear functions, linear programming requires them to be modelled and linearized. To facilitate its reproducibility, the linearization methods of all the nonlinear functions required for the modelling of the plant are detailed.

2. Materials and methods

Throughout this section, an hourly-based MILP model is developed for simultaneously optimizing the configuration, sizing and operation of thermal energy plants of residential buildings in the project phase. In order to compare the results obtained, depending on the objective function, three different perspectives are presented: two uni-objective optimization models —economic and environmental— and a

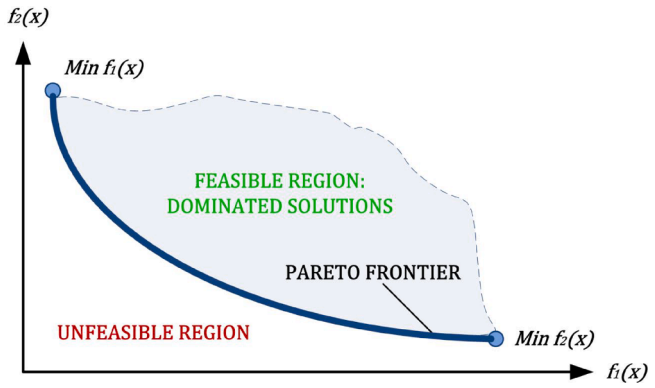

Fig. 1. Pareto Front.

multicriteria optimization.

In uni-objective models, one objective is minimized or maximized subject to constraints which contain information about the configuration of the plant, the characteristics of the technologies, the energy supply and the normative in force. In order to model and take decisions about complex situations —for instance, the technologies installed and their operation, the charging or discharging of the TES or the sale or purchase of electricity— MILP problems include integer and binary variables. Furthermore, linear programming requires a wide variety of real situations that meet the non-linear equations to be modelled; so linearization methods are used to obtain linear functions that correctly represent the non-linear behaviour of thermal systems.

The summation notation of the objective function in linear-programming is the following:

$$Min\ f(x) = \sum_j c_j \cdot x_j \tag{1}$$

Subject to the linear equality and inequality constraints:

$$\sum_j a_{ij} \cdot x_j \leq b_i \tag{2}$$

With non-negative variables:

$$x_j \geq 0 \tag{3}$$

where c_j, a_{ij} and $b_i$are constant and x_j corresponds to decision variables.

Regarding multi-criteria optimization, the Pareto optimization approach is used to obtain a set of optimal solutions when multiple conflicting objectives are considered. Pareto efficiency represents a specific state of allocation, which is based on the idea that it is impossible to improve a preference criterion without making another one worse. Thus, a set of non-dominated solutions is obtained, named the Pareto Front (Fig. 1). One solution dominates another when it is strictly better on at least one objective and not worse on any of them, so there is no solution outside the Pareto Front that provides better results than those included in it. The uni-objective perspective constitutes one of the end points of the optimal solution spectrum. For example, in a multi-criteria perspective where both overall cost and environmental impact are considered, one end-point represents the minimum cost solution, whereas the other is the solution corresponding to the minimum environmental impact.

In order to solve multi-objective optimization problems, both the weighted-sum method and the epsilon-constraints method are used. The weighted-sum method allows optimal solutions to be obtained through an approach based on a single objective function. For that purpose, each objective is multiplied by a user-defined weight, obtaining a single point which represents the multi-objective optimum. This method, widely used due to its simplicity, since it allows a multi-objective problem to be transformed into a uni-objective one, has a high sensitivity to the selection of weight coefficients. The epsilon-constraints method is used to avoid the high degree of subjectivity. It consists of optimizing one objective, while the others are converted into additional parametric constraints. The values selected as upper limits in the parametric constraints are obtained by means of the equidistant epsilon-constraints method, where the difference between the minimum and maximum values of the objective function converted into constraint is divided into equidistant points [22]. By the application of this method, the Pareto Front of the problem is obtained.

For a bi-objective problem, the objective function is the minimization of the *f(x)* function:

$$Min\ f(x) = \{f_1, f_2\} \tag{4}$$

By applying the epsilon-constraints method:

$$Min\ f_1(x) \tag{5}$$

$$Subject\ to: f_2(x) \leq \varepsilon_j \tag{6}$$

$$Lim_{low} \leq \varepsilon_j \leq Lim_{upp} \tag{7}$$

where f_1 and f_2 are uni-objective functions.

The optimal solution relies on repeatedly solving this model for different values of ε_j within the interval (Lim_{low} – Lim_{upp}). Thus, the Pareto Front is generated, which will be used later to select the multi-criteria optimal configuration.

$$\varepsilon_j = Lim_{low}, \varepsilon_1, \varepsilon_2, \cdots, Lim_{upp} \tag{8}$$

2.1. Selection of representative days

The energy analysis of buildings and their installations are usually carried out for a minimum period of one year. This is due to the fact that the sizing and operation of thermal installations in buildings have a temporary dependence. For instance, energy demands have great daily and seasonal fluctuations —which are mainly due to climatic conditions and dwellers' behaviour—, while the efficiency of some devices and technologies can also be affected by the weather and electricity tariffs with hourly discrimination are divided into different consumption periods throughout the day.

Regarding the optimization time period, an hourly basis is generally used for the energy analysis of buildings in most cases; whereas a sub-hourly basis is selected to analyse the transient behaviour, such as the charging and discharging of thermal energy systems or the starting and shutdown processes [23]. Nevertheless, carrying out an hourly-based MILP optimization considering the annual behaviour of hybrid installations leads to high computational costs. This calculation time increases linearly with the number of constraints, but exponentially with the number of variables, and the resolution of large-scale problems in a reasonable time becomes unfeasible.

Furthermore, in the optimization of hybrid systems, a different time basis is used depending on the constraint. Thus, some constraints related to legal requirements have an hourly basis: minimum energy efficiencies, minimum percentage of renewable contribution, minimum primary energy savings, etc. In other cases, the hourly operation is dependent on the state of the previous hour, for instance, thermal energy storage, start-up and shutdown processes, etc. As a consequence of using constraints of a different time basis, the annual optimum is not obtained as the summation of the hourly optimums, thus considerably increasing the calculation time.

For these reasons, the size of the problem has to be reduced by selecting a few representative days. The number of representative days has to ensure reliable results and fit the annual values of the model, while also decreasing the computational time.

Different methods have been used for the selection of representative days in distributed generation systems, from 3 representative days, where hourly and seasonal variations (winter, summer, spring-autumn) of the thermal demands are taken into account [24], to 8 representative

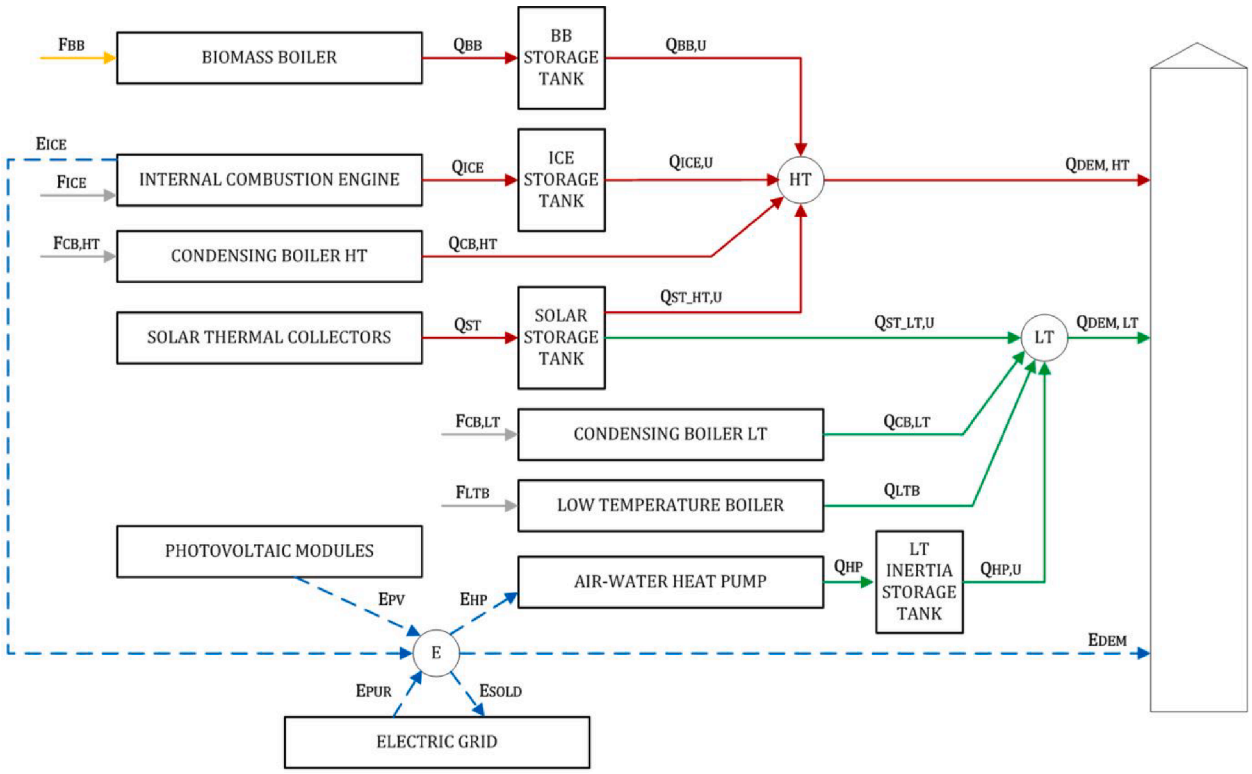

Fig. 2. Superstructure.

days, considering four seasons and 2 representative days per season [25], 12 representative days, one for each month of the year [26], or 24 days per year, 2 representative days per month, where working days and holidays are differentiated [12]. In other studies, the days of maximum demand for heating and cooling are included as representative days [27], or graphic methods based on the reproduction of the monotonic demand curve for the defined representative days are used [28].

In this paper, the method proposed for the selection of representative days is based on choosing one representative day that represents the average daily demand for every month. In addition, the day of maximum heating demand is considered as a representative day. Thus, for the domestic hot water (DHW) and electricity demands, as well as for climate data —such as the ambient temperature or solar radiation—, 12 representative days are considered —a daily profile per month—, whereas 13 day-types have been selected in order to represent the heating demand.

In the case of the heating demand, the representative day of each month is calculated by means of the Chebyshev theorem, which establishes that the average vector (centroid) of the group is the element that presents the minimum distance with respect to the other elements of the data set. Unlike the medoid, the centroid is not an object of the data set. Hence, the month with the peak demand day is represented by two representative days: the maximum demand day and the average day of the remaining days of the month, without including the maximum demand day. Thus, both peak demand and annual demand values are kept.

In order to validate the method proposed for selecting representative days, a graphic method based on the monotonic demand curve is used. The simulated monotonic demand curve is compared with the monotonic demand curve reproduced from the representative days, which is defined considering the number of times that each representative day is repeated throughout the year.

2.2. Definition of the superstructure

The superstructure, which includes different technologies used nowadays in thermal and electrical generation plants, is defined in this section. The aim is to obtain the optimal synthesis according to the optimization criteria (economic, environmental and multi-objective) and so compare the obtained results with the real thermal plant.

For this, it is necessary to define the technologies susceptible to being installed and to carry out an exhaustive bibliographic review in order to determine the technical features, cost and environmental impact of each of them, as well as the functions which relate these aspects to the nominal power. These relations are commonly nonlinear, so they have to be linearized by applying different linearization methods. Since the objective of this study is to get a general approximation which allows the different technologies to be compared and the technical, economic and environmental feasibility of the hybrid systems to be determined, the devices are modelled as a “black box”, which is a suitable approach for this study [29].

The superstructure (Fig. 2) is divided into two temperature levels according to the temperature of the terminal units and the DHW demand: high temperature (HT) for 60–80 °C and low temperature (LT) for 35–55 °C. For DHW generation, a minimum temperature of 60 °C is required in DHW storage to ensure health conditions [30]. For this reason, it is necessary to install any high temperature generation system that allows this temperature level to be reached. As far as heating demand is concerned, the terminal units installed can operate at HT (conventional radiators) or at LT (low temperature radiators or radiant floor). The type of terminal unit is a variable in the optimization model, which will stabilize –for the case analysed– the optimal temperature of the terminal systems. All the terminal units installed in the building are the same and operate at the same temperature; thus, the installation of HT generation systems for heating would exclude the installation of LT generation systems for this purpose, and vice versa.

The technologies considered in the superstructure are the most commonly used in the residential sector [31]. HT generation includes biomass boilers (BB), alternative internal combustion engines fed by natural gas (ICE), natural gas condensing boilers operating at high temperature (CB_{HT}) and solar thermal collectors (ST_{HT}). Within LT

Table 1
Nomenclature of sizing variables.

Technology	BIN_k	Y_{k_NOM}	Unit of Y_{k_NOM}
Biomass Boiler	BB	$\dot{Q}_{BB\_NOM}$	kW
Condensing Boiler	CB	$\dot{Q}_{CB\_NOM}$	kW
Low Temperature Boiler	LTB	$\dot{Q}_{LTB\_NOM}$	kW
Internal Combustion Engine	ICE	$\dot{E}_{ICE\_NOM}$	kW
Solar Thermal collectors	ST	S_{ST}	m^2
Air-water Heat Pump	HP	$\dot{Q}_{HP\_NOM}$	kW
Photovoltaic modules	PV	$\dot{E}_{PV\_NOM}$	W
Thermal Energy Storage	TES	V_{TES}	l

generation, solar thermal collectors (ST_{LT}), natural gas condensing boilers (CB_{LT}), natural gas low temperature boilers (LTB) and air-to-water heat pumps (HP) are considered.

Due to the efficiency requirements for heat generation systems, condensing boilers are considered for both temperature levels when natural gas is used as the fuel. Low temperature boilers, which have a high efficiency when operating at LT, have been excluded from HT technologies, since their use is not focused on this temperature level. As shown in Fig. 2, instead of installing a single condensing boiler capable of supplying the demand at both temperature levels, the possibility of installing a condensing boiler for each temperature level is considered. Even though this proposal implies greater investment, it offers great advantages with respect to the other one: better adjustment between supply and demand, simplification of the hydraulic installation and higher overall efficiencies.

In addition, four TES systems are susceptible to being installed, as shown in the superstructure diagram. Two of them are necessary for the HT level, due to the high inertia of the BB and CHP systems; another one for the ST technology, which requires its own storage system; and the last one at LT for the HP. Different TES systems have to be installed for different temperature levels; nevertheless, a joint tank could be used for the HT level, without distinguishing between the BB and ICE systems. The use of differentiated systems is justified by the necessity to determine the useful heat provided by the ICE in order to ensure compliance with the high efficiency cogeneration regulation. In all cases, the TES systems are arranged in parallel with the generation systems, with the possibility of simultaneous charging and discharging. This is the optimal configuration for a TES arrangement, as justified in previous works by the authors using linear programming [32] and simulation [33].

Furthermore, such electricity generation systems as micro-CHP engines (ICE) –which are also used for thermal generation at HT– and photovoltaic panels (PV) are analysed. The generated electricity can be self-consumed if it is lower than the electricity demand of the building (users' consumption and heat pump consumption in the case of this being installed), or it can be poured into the grid. The electricity consumption of pumps and fans in distribution and generation is not considered, due to the fact that the variation of this consumption between configurations can be assumed negligible compared to the overall energy consumption of the plant.

This superstructure allows different design options to be analysed simultaneously and the optimal one to be determined. The computation time depends on the optimization model, the potential of the software selected and the problem definition.

In this case, the optimization model is developed in OpenSolver software, which supports the Open Source CBC (COIN-OR Branch and Cut) linear and mixed-integer programming solver implemented as a complement of Excel VBA [34]. This solver can solve large-scale MILP models, the computational time required being similar to its commercial equivalents [35]. The advantage of using OpenSolver instead of commercial solvers is that the software environment is widely known by engineers and researchers, which encourages the spread of its use. Apart from this, the price of commercial solvers cannot always be justified by the benefits of reporting the optimization models [9].

2.3. Optimization model of combined generation

In this section, the proposed optimization model is carried out. First, the objective functions and constraints of both economic, environmental and multi-objective optimization models are all presented. Then, energy balances in energy supply nodes and technologies considered in the superstructure are obtained. Finally, the legal constraints related to the energy savings required or the contribution of renewable energy systems have to be defined. As the normative depends on the country where the installation is located, these constraints are presented within the case study,

2.3.1. Economic optimization

The principal aim is to determine the optimal synthesis, sizing and operation of an energy generation plant which minimize its overall cost, while also ensuring the supply of thermal and electric energy. The target of the optimization problem is to minimize the objective function, which is represented by the overall cost of the plant. This cost comprises fixed costs (C_{INV}) and variable costs ($C_{O\&M}$).

$$Min\ C_{TOT} = C_{INV} + C_{O\&M} \tag{9}$$

The fixed costs include annual investment costs —calculated for each technology k as the product of the capital recovery factor (CRF_k) and the investment cost C_k—, and maintenance costs based on a percentage of the investment (C_{FM}).

$$C_{INV} = \sum_k \left(CRF_k \cdot C_k + C_{FM,k}\right) \tag{10}$$

where the CRF factor is calculated as follows:

$$CRF_k = \frac{i\cdot(1+i)^{n_k}}{(1+i)^{n_k}-1} \tag{11}$$

i being the effective annual interest rate and nk the lifetime of each technology.

The investment cost is calculated by considering the cost curve defined from the sizing variable (Y_{k_NOM}) of each technology. Since a technology may or may not be installed, binary variables (BIN_k) are used for modelling this possibility. Thus, the binary variable of a certain technology will be 1 when this technology is installed —the investment cost is calculated by using the cost function ($C(Y_{k\_NOM})$)—; whereas the value will be 0 when it is not installed —and the investment cost is 0. This problem represents a non-linear IF statement that has to be linearized. The linearization method proposed in this model is the big-M method, which consists of taking a high value constant (M) that allows functions to be discriminated and lets the constraint move outside the limits of the region inscribed by the problem constraints [36].

$$C_k \le 0 + M\cdot BIN_k \tag{12}$$

$$C_k \ge 0 - M\cdot BIN_k \tag{13}$$

$$C_k \le C(Y_{k\_NOM}) + M\cdot(1 - BIN_k) \tag{14}$$

$$C_k \ge C(Y_{k\_NOM}) - M\cdot(1 - BIN_k) \tag{15}$$

The nomenclature related to the sizing and binary variables of each technology is summarized in Table 1.

The annual operation and maintenance cost $C_{O\&M}$ is calculated as the product of the sum of the hourly (h) operation and maintenance costs of each representative day (d) and the number of times each representative day is repeated during a year $ntd(d)$. These costs include fuel and electricity consumption —such as the natural gas consumption in condensing and low temperature boilers and in the micro-CHP unit (c_{NG}) —, the cost of pellet consumption in the biomass boiler (c_{BB}), the cost of the electricity purchased from the grid (c_{EPUR}) and the maintenance cost, which is a function of the operation variables, as in the case of micro-CHP units, whose maintenance cost ($c_{VM,ICE}$) depends on the power

generation.

$$C_{O\&M} = \sum_{d}\sum_{h} C_{O\&M}(d,h)\cdot ntd(d) \tag{16}$$

$$\begin{aligned} C_{O\&M}(d,h) = {} & c_{NG}\cdot\left(F_{CB,HT}(d,h) + F_{ICE}(d,h) + F_{CB,LT}(d,h) + F_{LTB}(d,h)\right) \\ & + c_{BB}\cdot F_{BB}(d,h) + c_{EPUR}(d,h)\cdot E_{PUR}(d,h) \\ & - c_{ESOLD,k}(d,h)\cdot E_{SOLD,k}(d,h) + c_{VM}(d,h)\cdot E_{ICE}(d,h) \end{aligned} \tag{17}$$

2.3.2. Environmental optimization

The objective function in environmental optimization consists of minimizing the GHG emissions — measured in carbon dioxide equivalent ($CO_{2\text{-eq}}$)—, including the emissions generated in the manufacturing of the equipment (CO_{2_FIX}) and during the operation of the plant ($CO_{2\_O\&M}$).

$$Min\ CO_{2\_TOT} = CO_{2\_FIX} + CO_{2\_O\&M} \tag{18}$$

The fixed term CO_{2_FIX} is calculated as the hourly sum of the product between the environmental amortization factor FAM_{ENV} of each technology k and the emissions generated during its manufacturing [37].

$$CO_{2\_FIX} = \sum_{k}\left(FAM_k\cdot CO_{2,k}\right) \tag{19}$$

The environmental amortization factor *FAM* is calculated as the inverse of the useful life of each technology, considering the same environmental impact for every year of its useful life.

$$FAM_k = 1/n_k \tag{20}$$

Under the same assumptions considered for the investment cost, the manufacturing $CO_{2\text{-eq}}$ emissions of each technology are calculated as follows:

$$CO_{2,k} \le 0 + M\cdot BIN_k \tag{21}$$

$$CO_{2,k} \ge 0 - M\cdot BIN_k \tag{22}$$

$$CO_{2,k} \le CO_2(Y_{k\_NOM}) + M\cdot(1 - BIN_k) \tag{23}$$

$$CO_{2,k} \ge CO_2(Y_{k\_NOM}) - M\cdot(1 - BIN_k) \tag{24}$$

Regarding the $CO_{2\text{-eq}}$ emissions during operation, the emissions related to both energy resource and consumption are considered. Taking into account the fact that no $CO_{2\text{-eq}}$ is emitted during the operation of renewable technologies, the GHG emissions during the plant operation correspond to those produced by the combustion of natural gas, the preparation and transport of biomass and the generation of supply electricity.

$$\begin{aligned} CO_{2\_O\&M}(d,h) = {} & co_{2,NG}\cdot\left(F_{CB,HT}(d,h) + F_{ICE}(d,h) + F_{CB,LT}(d,h)\right. \\ & \left. + F_{LTB}(d,h)\right) + co_{2,BB}\cdot F_{BB}(d,h) + co_{2,EPUR}(d,h)\cdot E_{PUR}(d,h) \end{aligned} \tag{25}$$

2.3.3. Multi-criteria optimization

Nowadays, the design of thermal installations for buildings should be focused on sustainable technologies, which include both economic and environmental aspects. The ideal technology should be that whose cost and environmental impact are both minimum. However, these objectives are usually opposing; therefore, the minimum cost technologies produce greater environmental impact and vice versa. For considering the simultaneous optimization of both conflicting objectives, the Pareto Front explained above is obtained. Thus, the optimal set of design and operational variables that achieves the double objective of reducing environmental impact and economic cost is depicted.

The epsilon-constraints method is applied to simultaneously minimize cost and GHG emissions:

$$Min\ C_{TOT} \tag{26}$$

$$Subjectto: CO_{2\_TOT} \le \varepsilon_j \tag{27}$$

$$Minimum\ CO_{2\_TOT} \le \varepsilon_j \le Maximum\ CO_{2\_TOT} \tag{28}$$

In this case, the environmental optimum (maximum cost) is the lower bound (Lim_{low}) and the GHG emissions corresponding to the economic optimum (maximum environmental impact) is the upper bound (Lim_{upp}).

2.3.4. Supply of thermal demand

The thermal demand is the sum of the heating and DHW demands.

$$Q_{DEM}(d,h) = Q_{HEAT}(d,h) + Q_{DHW}(d,h) \tag{29}$$

In the case of DHW demand, this is supplied at HT to avoid the growth of Legionella bacteria, as previously stated. The heating demand, for its part, can be covered by devices operating at HT when conventional radiators are installed, or at LT when low temperature radiators or radiant floor are installed. For this reason, the thermal demand at HT is the sum of the DHW demand and the heating demand when the latter is supplied by means of HT technologies. In order to determine whether the terminal units operate at high or low temperature, a binary variable $HEAT_{HT}$ is used, whose value will be 1 for HT terminal units and 0 for LT ones. The value of $HEAT_{HT}$ is determined by the resolution of the model. The cost of the terminal units is not included in this study.

$$Q_{DEM\_HT}(d,h) = Q_{DHW}(d,h) + Q_{HEAT,HT}(d,h)\cdot HEAT_{HT} \tag{30}$$

$$Q_{DEM\_LT}(d,h) = Q_{HEAT,LT}(d,h)\cdot(1 - HEAT_{HT}) \tag{31}$$

$$HEAT_{HT}\ \ bin \tag{32}$$

The hourly supply at HT is obtained by applying an energy balance in the node HT. As shown in Fig. 2, the thermal demand at HT can be met through the heat generated by the CB_{HT} ($Q_{CB,HT}(d,h)$) and the useful heat —discharged from the TES— of the BB ($Q_{TES,BB}(d,h)$), ICE ($Q_{TES,ICE}(d,h)$) and ST_{HT} ($Q_{ST,HT}(d,h)$).

$$Q_{DEM.HT}(d,h) = Q_{TES,BB}(d,h) + Q_{TES,ICE}(d,h) + Q_{CB,HT}(d,h) + Q_{ST,HT}(d,h) \tag{33}$$

Likewise, the energy balance is applied in node LT to determine the hourly supply at LT. This can be provided through the heat produced by the CBLT ($Q_{CB,LT}(d,h)$) and the LTB ($Q_{LTB}(d,h)$), as well as by the useful heat of the ST_{LT} ($Q_{ST,LT}(d,h)$) and HP ($Q_{TES,HP}(d,h)$).

$$Q_{DEM\_LT}(d,h) = Q_{ST,LT}(d,h) + Q_{CB,LT}(d,h) + Q_{LTB}(d,h) + Q_{TES,HP}(d,h) \tag{34}$$

2.3.5. Supply of electricity demand

In order to decide which electricity generation technologies should be installed, as well as the electric energy required and poured into the grid, the energy balance in node E is carried out:

$$E_{PV}(d,h) + E_{ICE}(d,h) + E_{PUR}(d,h) = E_{HP}(d,h) + E_{SOLD}(d,h) + E_{DEM}(d,h) \tag{35}$$

where E_{PUR} is the electricity purchased from the grid and E_{SOLD} the electricity sold. As can be seen in Eq. (35), electricity cannot be purchased and sold at the same time. This is an if-else decision; so, if the power generation is greater than the electricity demand, the surplus electricity is poured into the grid; otherwise, electricity is purchased from the grid. This situation requires the use of binary variables *PUR(d,h)* and *SOLD(d,h)*, which determine when the electricity is purchased or sold, respectively. In order to linearize the if-else decision, a big M method is applied.

$$\begin{aligned} E_{PUR}(d,h) \le {} & E_{HP}(d,h) + E_{DEM}(d,h) - E_{PV}(d,h) - E_{ICE}(d,h) + (1 \\ & - PUR(d,h))\cdot M \end{aligned} \tag{36}$$

$$E_{PUR}(d,h) \geq E_{HP}(d,h) + E_{DEM}(d,h) - E_{PV}(d,h) - E_{ICE}(d,h) - (1 - PUR(d,h))\cdot M \quad (37)$$

$$E_{SOLD}(d,h) \leq E_{PV}(d,h) + E_{ICE}(d,h) - E_{HP}(d,h) - E_{DEM}(d,h) + (1 - SOLD(d,h))\cdot M \quad (38)$$

$$E_{SOLD}(d,h) \geq E_{PV}(d,h) + E_{ICE}(d,h) - E_{HP}(d,h) - E_{DEM}(d,h) - (1 - SOLD(d,h))\cdot M \quad (39)$$

$$PUR(d,h)\ bin \quad (40)$$

$$SOLD(d,h)\ bin \quad (41)$$

$$PUR(d,h) + SOLD(d,h) = 1 \quad (42)$$

2.3.6. Energy balances of technologies

In this section, the energy balances of the considered technologies are defined and linearized. The variables that are optimized by the proposed model are related to the installation possibility of each technology, its size and its operation mode.

Regarding size, the installed sizing variable (Y_{k_NOM}) —the nominal power for boilers, HP and PV, the volume for TES systems and the surface for solar thermal collectors—depends on the devices available in the market. When the cost-sizing variable curve is defined, there is a minimum value of this, for which one technology is commercialized. The maximum value corresponds to the peak demand or space limits. Thus, if any technology is installed ($BIN_k = 1$), the Y_{k_NOM} installed has to be greater than or equal to this minimum value Y_{k_MIN} and lower than the maximum value Y_{k_MAX}. Otherwise, ($BIN_k = 0$) and the Y_{k_NOM} installed has to be 0.

$$Y_{k\_NOM} \geq Y_{k\_MIN}\cdot BIN_k \quad (43)$$

$$Y_{k\_NOM} \leq Y_{k\_MAX}\cdot BIN_k \quad (44)$$

The operation functions are defined below, taking into account the distinctive features of each technology.

2.3.6.1. Boilers. These equations are applied to both natural gas-fired condensing and low temperature boilers and biomass-fired boilers. In other words, the *B* binary variable is used, which represents any of the considered boilers. Regarding operation, the heat generated by a boiler has to be lower than or equal to the thermal energy supplied during one hour at nominal conditions ($\dot{Q}_{B\_NOM}$) when this technology operates, or zero if that is not the case. An installed technology can operate or not, so binary variables —*BB(d,h), CB_{HT}(d,h), CB_{LT}(d,h)* and *LTB(d,h)*— are used to determine the operation of each technology. As mentioned above, a binary variable *B(d,h)* is used in the equations to represent the operation (or not) of any boiler.

$$Q_B(d,h) \leq B(d,h)\cdot\dot{Q}_{B\_NOM}\cdot t \quad (45)$$

On the other hand, as the size of each technology ($\dot{Q}_{B\_NOM}$ installed) is unknown, $\dot{Q}_{B\_NOM} \cdot B(d,h)$ is a product of variables. To linearize this function, it is considered that the thermal energy supplied by a boiler in hour *h* of day *d* has to be 0 when this technology is not installed; whereas it has to be lower than the nominal power and greater than 0 for the thermal energy provided by the first stage of a modulating boiler, if the technology is installed. For instance, if a modulating burner starts from a percentage (PL_{B_MIN}) of the nominal thermal power, $Q_B(d,h)$ has to be equal to or greater than the power provided at this minimum part-load ratio, when the device operates. This is linearized by means of the big-M method. The fuel consumption, for its part, is calculated considering an average thermal efficiency for each technology.

$$Q_B(d,h) \leq 0 + B(d,h)\cdot M \quad (46)$$

$$Q_B(d,h) \geq 0 - B(d,h)\cdot M \quad (47)$$

$$Q_B(d,h) \leq \dot{Q}_{B\_NOM}\cdot t \quad (48)$$

$$Q_B(d,h) \geq PL_{B,MIN}\cdot\dot{Q}_{B\_NOM}\cdot t - (1 - B(d,h))\cdot M \quad (49)$$

$$B(d,h)\ bin \quad (50)$$

$$F_B(d,h) = \frac{Q_B(d,h)}{\eta_B} \quad (51)$$

2.3.6.2. Internal combustion engines. For modelling micro-CHP devices based on ICE, no modulating units are taken into account, since most of the commercialized ICE-based micro-CHP units do not have the possibility of operating at partial load [38]. A binary variable, *ICE(d,h)*, is defined to determine if this technology operates in case of being installed ($ICE = 1$).

$$ICE, ICE(d,h)\ bin \quad (52)$$

$$ICE(d,h) \leq ICE \quad (53)$$

The thermal energy produced by the engine is the product of the thermal energy provided for one hour at nominal thermal power ($\dot{Q}_{ICE\_NOM}$) and the binary variable *ICE(d,h)*. This is a product of two variables that has to be linearized by means of the Big M method. Thus, when the engine operates, $Q_{ICE}(d,h)$ has to be equal to the nominal thermal energy and, otherwise, its value has to be 0.

$$Q_{ICE}(d,h) \leq M\cdot ICE(d,h) \quad (54)$$

$$Q_{ICE}(d,h) \geq -M\cdot ICE(d,h) \quad (55)$$

$$Q_{ICE}(d,h) \leq \dot{Q}_{ICE\_NOM}\cdot t + M\cdot(1 - ICE(d,h)) \quad (56)$$

$$Q_{ICE}(d,h) \geq \dot{Q}_{ICE\_NOM}\cdot t - M\cdot(1 - ICE(d,h)) \quad (57)$$

The nominal thermal power is calculated from the nominal electricity power —which is the parameter that defines cogeneration units— and thermal and electric efficiencies. Since the installed nominal power is unknown, efficiency mean values are considered, which are defined considering commercialized natural gas fuelled ICE engines.

$$F_{ICE}(d,h) = E_{ICE}(d,h)/\eta_E \quad (58)$$

$$Q_{ICE}(d,h) = E_{ICE}(d,h)\cdot\eta_Q/\eta_E \quad (59)$$

$$\dot{F}_{ICE\_NOM} = \dot{E}_{ICE\_NOM}/\eta_E \quad (60)$$

$$\dot{Q}_{ICE\_NOM} = \dot{E}_{ICE\_NOM}\cdot\eta_Q \Big/ \eta_E \quad (61)$$

According to the European Directive on Energy Efficiency 2012/27/EU (EED) [39], micro-CHP is defined as cogeneration with a maximum electric capacity below 50 kWe. Since only micro-CHP technologies are considered, the installed nominal electric power has to be lower than this value.

$$\dot{E}_{ICE\_NOM} \leq 50 \quad (62)$$

2.3.6.3. Solar thermal collectors. The type of collector selected for the analysis of this technology is flat plate solar collectors, as they are the most commonly used in the residential sector. The hourly solar global incident radiation on the collector surface (*G*) is obtained from the meteorological data of the building location.

The radiation absorbed by the solar collector, $R_{abs}(d,h)$, is calculated as follows:

$$R_{abs}(d,h) \leq \eta_{ST}(d,h)\cdot(1 - \sigma)\cdot G(d,h) + M\cdot ST \quad (63)$$

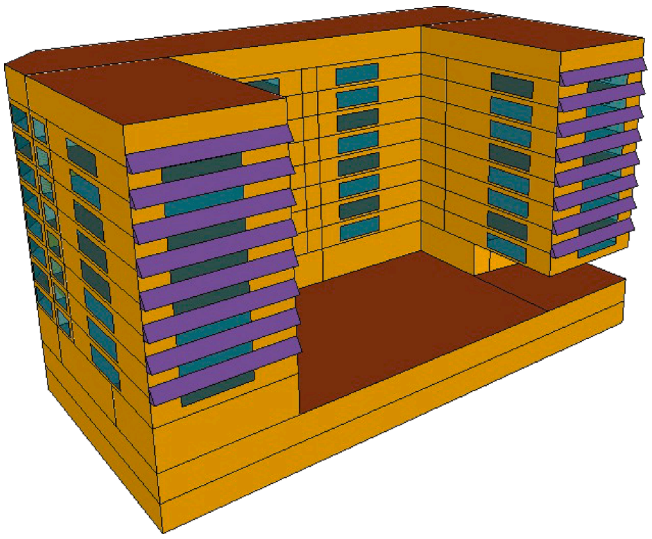

Fig. 3. Building model.

$$R_{abs}(d,h) \geq \eta_{ST}(d,h)\cdot(1-\sigma)\cdot G(d,h) - M\cdot ST \tag{64}$$

$$ST \ bin \tag{65}$$

where η_{ST} is the thermal efficiency —obtained from the hourly ambient temperature, the hourly incident radiation and the mean temperature in the collector—,σ is the value of orientation and inclination losses, $G(d,h)$ is the hourly incident radiation and ST is the binary variable which defines whether the technology is installed or not.

Heat generated by the solar collectors is the product of the absorbed heat $R_{abs}(d,h)$ and the installed surface S_{ST}.

$$Q_{ST}(d,h) = R_{abs}(d,h)\cdot S_{ST} \tag{66}$$

Moreover, the ratio between the solar tank volume and the solar collector surface, $r_{V\text{-}S}$, must be between a range of values.

$$V_{STO,ST}(d,h) = r_{V-S}\cdot S_{ST} \tag{67}$$

2.3.6.4. Air-water heat pumps. Two binary variables, HP and $HP(d,h)$, are defined for this heat pump. The first represents whether this technology is installed, while the second refers to the operation of this technology at instant (d,h) if installed. These two variables are related to each other, so the device can operate ($HP(d,h) = 1$) only when it is installed ($HP = 1$).

$$HP(d,h) \leq HP \tag{68}$$

$$HP, HP(d,h) \ bin \tag{69}$$

The thermal power produced by the heat pump will be zero when the equipment does not operate or, on the contrary, it will operate between the minimum part-load ratio and full load. This if-else problem can be solved by the $HP(d,h)$ binary variable and the big-M method. Thus, if $HP(d,h)$ is equal to unit, HP operates between the modulation range ($PL_{HP\_MIN}\cdot Q_{HP\_NOM} \leq Q_{HP(d,h)} \leq Q_{HP\_NOM}\cdot t$); otherwise, ($Q_{HP}(d,h) = 0$) the heat generation is zero.

$$Q_{HP}(d,h) \leq M\cdot HP(d,h) \tag{70}$$

$$Q_{HP}(d,h) \geq -M\cdot HP(d,h) \tag{71}$$

$$Q_{HP}(d,h) \leq \dot{Q}_{HP\_NOM}\cdot t + M\cdot(1 - HP(d,h)) \tag{72}$$

$$Q_{HP}(d,h) \geq PL_{HP\_MIN}\cdot\dot{Q}_{HP\_NOM}\cdot t - M\cdot(1 - HP(d,h)) \tag{73}$$

The consumption of electricity in the heat pump $E_{HP}(d,h)$ is calculated as the ratio between the nominal heat and the coefficient of performance (COP), whose value depends on the return temperature of water and the ambient temperature.

$$E_{HP}(d,h) = Q_{HP}(d,h)/COP_{HP}(d,h) \tag{74}$$

2.3.6.5. Photovoltaic panels. The electricity generation is determined from the hourly production profiles defined by the Royal Decree 413/2014 [40], as the product of the nominal power installed and the hourly operation factor fo_{PV}.

$$E_{PV}(d,h) = \dot{E}_{PV,NOM}\cdot t\cdot fo_{PV}(d,h) \tag{75}$$

2.3.6.6. Thermal energy storage. According to the superstructure (Fig. 2), the installation of TES is conditioned by the installation of BB, ICE, ST and HP generation systems. For the configuration of TES arranged in parallel with the generation system and considering the possibility of simultaneous charging and discharging [32], the energy balance of TES is applied as follows:

$$Q_{STO}(d,h) = Q_{STO}(d,h-1) + Q_{CHAR}(d,h) - Q_{DISCH}(d,h) - Q_{LOSS}(d,h) \tag{76}$$

Where $Q_{STO}(d,h)$ is the heat stored every hour, $Q_{STO}(d,h\text{-}1)$ is the heat stored in the previous instant, $Q_{CHAR}(d,h)$ and $Q_{DISCH}(d,h)$ are, respectively, the thermal energy charged and discharged, and $Q_{LOSS}(d,h)$ represents the thermal losses calculated as a percentage of the thermal energy content in the previous instant.

$$Q_{LOSS}(h) = PCT_{LOSS}\cdot Q_{STO}(d,h-1) \tag{77}$$

Due to the fact that the generation systems are directly connected to the TES, all the thermal energy produced $Q_k(d,h)$ is charged into the tank. As aforementioned, the useful heat supplied by each technology $Q_{k,U}(d,h)$ is the thermal energy discharged from its corresponding tank.

$$Q_{CHAR}(d,h) = Q_k(d,h) \tag{78}$$

$$Q_{DISCH}(d,h) = Q_{k,U}(d,h) \tag{79}$$

In the case of ST, the thermal energy discharged is distributed to high and low temperature circuits:

$$Q_{DISCH}(d,h) = Q_{ST,HT}(d,h) + Q_{ST,LT}(d,h) \tag{80}$$

Apart from this, the $Q_{DISS,ST}(d,h)$ term is included within the losses in the solar tank. This term corresponds to the heat losses to the surroundings, which are dissipated through an air heater installed at the exit of the collectors to prevent the overheating of the solar circuit.

$$Q_{LOSS}(h) = PCT_{LOSS}\cdot Q_{STO}(d,h-1) + Q_{DISS,ST}(d,h) \tag{81}$$

On the other hand, the discharged energy cannot be greater than the heat content in the previous instant.

$$Q_{DISCH}(d,h) \leq Q_{STO}(d,h-1) \tag{82}$$

Furthermore, it is assumed that there is no heat stored in the initial instant. The heat stored at every instant must be lower than the maximum capacity of the TES, Q_{CAP}. If any particular technology was not installed, the energy produced, and consequently the energy stored and the capacity of the corresponding TES, would be zero.

$$Q_{STO}(d,0) = 0 \tag{83}$$

$$Q_{STO}(d,h) \leq Q_{CAP} \tag{84}$$

The maximum capacity (Q_{CAP})is related to the TES volume (V_{TES}) by the following equation:

$$V_{TES} = \frac{Q_{CAP}\cdot 3600}{cw\cdot\rho\cdot\Delta T} \tag{85}$$

where V_{TES} is the capacity of the inertia tank in litres, Q_{CAP} is the maximum capacity of the TES in kWh, cw is the specific heat in kJ/kg·K,

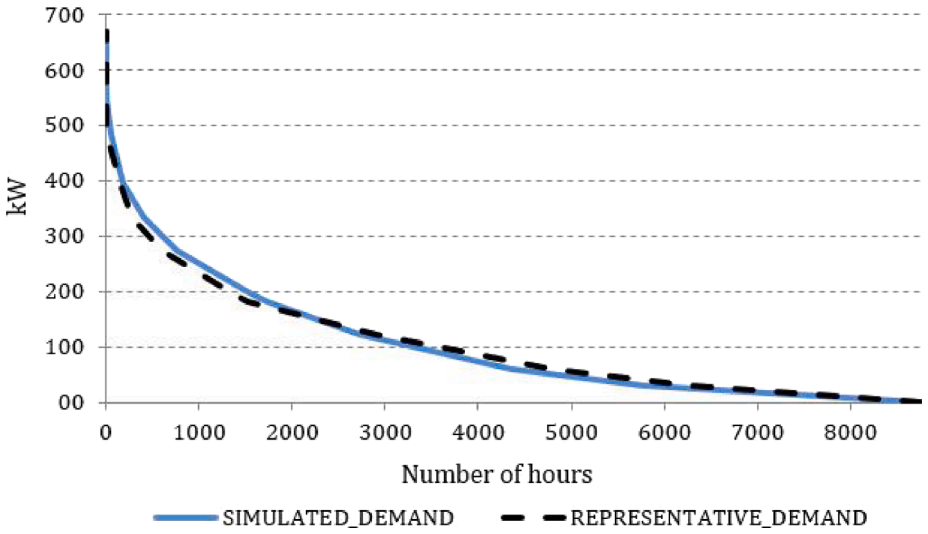

Fig. 4. Comparison between simulated and representative curve of thermal demand.

Table 2
Technical features of technologies.

Technology	n_k (years)	Y_{k_MIN}	Y_{k_MAX}	Unit of Y_{k_NOM}	Efficiency
BB	15	16	660	kW	$\eta_{BB,30}(LHV) = 90.3\%$; $\eta_{BB,100}(LHV) = 91.9\%$; $\eta_{BB,ave}(LHV)$: 91.1% ; $PL_{BB\_MIN} = 0.30$
CB	15	50	660	kW	$\eta_{CB_{HT}}(LHV) = 98.163 - 0.6015 \cdot PL$ (for $T_r = 60$ °C) $\eta_{CB_{HT},ave}(LHV)$: 97.8% $\eta_{CB_{LT}}(LHV) = 108.138 - 3.766 \cdot PL$ (for $T_r = 35$ °C) $\eta_{CB_{LT,ave}}(LHV)$: 106.0%
LTB	15	120	660	kW	$\eta_{LTB}(LHV) = 93.784 - 1.109 \cdot PL$ (for $T_r = 35$ °C) $\eta_{LTB,ave}(LHV)$: 93.2%
ICE	15	1	50	kW	$\eta_{ICE,E} = 21.188 \cdot \dot{E}_{ICE_{NOM}}^{0.116}$ $\eta_{ICE,Q} = 71.735 \cdot \dot{E}_{ICE\_NOM}^{-0.057}$ $\eta_{ICE,E,ave} = 60.3\%$; $\eta_{ICE,Q,ave} = 30.4\%$
ST	25	4	130	m^2	$\eta_{ST}(d,h) = \left(0.8057 - 6.0143 \cdot \frac{T_{ave} - T_{amb}(d,h)}{G(d,h)}\right)$ $\sigma = 6\%$; $r_{v-s} = 75\frac{l}{m^2}$; $T_{ave} = 45°C$
HP	20	21	660	kW	$COP_{HP}(d,h) = 0.09 \cdot T_{amb}(d,h) + 3.5514$ (for $T_r = 35$ °C) $PL_{HP\_MIN} = 0.08$ (8%)
PV	25	130	58,700	W	f_{op} (d,h)
TES	15	100	25,000	l	$PCT_{LOSS,HT} = 1\%$ (for $T_{STO} = 70$ °C) $PCT_{LOSS,LT} = 0.6\%$ (for $T_{STO} = 45$ °C) $\Delta T = 20$ °C

ρ is the density in kg/l, and ΔT is the temperature difference between top and bottom in the tank in K.

2.4. Case study

The selected residential building is a recently built multi-storey building located in a cold climate in the north of Spain, which includes 176 social dwellings. The characteristics of the building are included in Appendix A. The heating demand is calculated by means of the modelling and analysis of the building in the transient building energy simulation software Trnsys 17 (Fig. 3). For that, the characteristics of the building have to be determined: occupation, set-point temperatures, ventilation and infiltration rates, envelope properties, etc [41] (Appendix A). According to the hourly simulation results, the annual space heating demand is 600.5 MWh.

Regarding the DHW demand, this is calculated according to the Spanish Technical Building Code (CTE), which establishes that the daily consumption in dwellings is 28 l/(person·day) [42]. To determine the occupation of the dwellings, the minimum value of occupation established by the CTE is considered, which is a function of the total number of bedrooms. The DHW hourly consumption in litres is obtained from the product of the hourly and monthly multiplier factors [43] and the aforementioned daily consumption. These multiplier factors are shown in and in Appendix A. In order to determine the DHW demand in terms of energy, the cold water entering and the supply temperatures must be defined. The DHW supply temperature is assumed to be 60 °C, while for the cold-water temperature, the monthly average values provided by the CTE for the building location are used [42]. The calculated annual DHW demand is 289.6 MWh.

From the hourly heating and DHW demand, the monotonic curves can be calculated. In Fig. 4, the monotonic curve of the representative demand —calculated with 13 representative days— is compared to the monotonic curve obtained from the simulation results. As shown, the representative curve is correctly fitted to the simulated demand, the maximum hourly error being lower than 5%.

Regarding the electricity demand, this is calculated by means of the annual and daily profiles shown in and [44] in Appendix A, respectively, and supposing an average annual electricity demand of 3100 kWh for a dwelling unit in Vitoria-Gasteiz [45].

2.4.1. Technical, economic and environmental data

In this section, a literature review is presented to determine the

Table 3
Investment and maintenance costs.

Technology	Investment cost (€)		Maintenance cost (€/y)
BB	$C_{BB} = 197.61 \cdot \dot{Q}_{BB\_NOM} + 14504$	($R^2 = 0.9716$)	$0.04 \cdot C_{BB}$
CB	$C_{CB} = 39.42 \cdot \dot{Q}_{CB\_NOM} + 8772$	($R^2 = 0.9477$)	$0.095 \cdot C_{CB}$
LTB	$C_{LTB} = 15.16 \cdot \dot{Q}_{LTB\_NOM} + 4065$	($R^2 = 0.9864$)	$0.095 \cdot C_{LTB}$
ICE	$C_{ICE} = 5714.7 \cdot \dot{E}_{ICE\_NOM}^{0.6558}$	($R^2 = 0.9549$)	$0.028 \cdot E_{ICE}$
ST	$C_{ST} = 770.29 \cdot S_{ST} + 3445$	($R^2 = 0.9997$)	$0.051 \cdot C_{ST}$
HP	$C_{HP} = 285.34 \cdot \dot{Q}_{HP\_NOM} - 1422$	($R^2 = 0.9912$)	$0.064 \cdot C_{HP}$
PV	$C_{PV} = 0.2266 \cdot \dot{E}_{PV\_NOM} + 610$	($R^2 = 0.9393$)	$0.015 \cdot C_{PV}$
TES	$C_{TES} = 29.968 \cdot V_{TES}^{0.6382}$	($R^2 = 0.9587$)	$0.021 \cdot C_{TES}$

Table 4
Coefficients for linear approximation of ICE investment cost.

$E_{ICE,NOM}$ (kW)	a	b
0–1	5714.70	0
1–5	2676.37	3038.33
5–10	1889.93	6970.54
10–20	1488.78	10982.01
20–50	1119.16	18374.47

Table 5
Coefficients for linear approximation of TES investment cost.

Volume (l)	a	b
0–500	3.1635	0
500–1000	1.7601	701.69
1000–5000	1.1036	1358.3

technical characteristics of the considered technologies, their investment costs and the environmental impact during the manufacturing process. From generic data provided by the manufacturers, catalogues and experimental testing, the efficiency, cost and emission curves are defined and outlined in Tables 2, 3 and 6, respectively. Apart from this, the economic cost and the environmental impact of the different energy resources are also established.

The technical features of the equipment are summarized in Table 2. Within this information, the useful life of every technology, the sizing limits and the efficiency or loss functions are highlighted. As mentioned in Section 2.6, the minimum sizing value is that corresponding to commercialized devices used in collective installations for both space heating and DHW. On the other hand, its maximum value depends on the instantaneous maximum thermal power required in the case of BB, CB, LTB and HP, on the maximum surface available in the case of ST and PV, on the maximum value established for micro-CHP in ICE, and on the space of the boiler room that can be used for accumulation in the case of TES.

Regarding the available area for installing solar technologies, roof and south-east orientation façades are considered. As two different solar technologies can be installed, it has been established that ST collectors would be installed on the roof and PV panels would be integrated into the building façade —the maximum surface that can be installed being the actual one (422 m^2 with an installed power of 58.7 kW). Considering that ST panels would be installed on the inclined roof —with an inclination angle of 30° and south-east orientation with an azimuth of 7°—, the maximum surface available is 130 m^2. The minimum surface considered for a block of flats if solar thermal collectors are installed is 4 m^2 [46].

Table 6
GHG emissions of manufacturing.

Technology	Fabrication $CO_{2\text{-eq}}$ emissions (kg)	
BB	$CO_{2,BB} = 49.516 \cdot \dot{Q}_{BB\_NOM} + 1080$	($R^2 = 0.9694$)
CB	$CO_{2,CB} = 9.5207 \cdot \dot{Q}_{CB\_NOM} + 1576$	($R^2 = 0.9534$)
LTB	$CO_{2,LTB} = 10.934 \cdot \dot{Q}_{LTB\_NOM} + 1192$	($R^2 = 0.9889$)
ICE	$CO_{2,ICE} = 226.16 \cdot \dot{E}_{ICE\_NOM} + 1557$	($R^2 = 0.8868$)
ST	$CO_{2,ST} = 129.48 \cdot S_{ST} + 874$	($R^2 = 0.9999$)
HP	$CO_{2,HP} = 63.595 \cdot \dot{Q}_{HP\_NOM} + 3552$	($R^2 = 0.9626$)
PV	$CO_{2,PV} = 1508 \cdot \dot{E}_{PV\_NOM}$	($R^2 = 1.0000$)
TES	$CO_{2,TES} = 0.4505 \cdot V_{TES} + 646$	($R^2 = 0.9593$)

Furthermore, the generic efficiency and loss curves are obtained for every technology. As the generic data of the technologies are considered, the average thermal efficiencies are calculated according to the aforesaid curves. In the case of CB and LTB boilers, the efficiency curves were developed within the framework of the Defra Market Transformation Programme (MTB) [47]. These curves fit a polynomial equation which depends on the temperature of the return water and the load. In Table 3, the efficiency functions are defined for both HT and LT generation. Concerning BB, the efficiency of 166 devices is analysed in [48] for both 30% part-load ratio and full-load. Meanwhile, the thermal and electric efficiencies of ICE are determined in [49], where 59 ICE-based micro-CHP units are analysed.

In order to calculate the absorbed heat in ST, the value of the orientation and inclination losses (σ) and the efficiency ($\eta_{ST}(d,h)$) have to be determined. According to the CTE, the value of σ has to be lower than 10%, with a common setting being at 6% [50]. The $\eta_{ST}(d,h)$ is calculated from the hourly incident radiation $G(d,h)$ and the ambient temperature $T_{amb}(d,h)$ [46], whose values for the city of Vitoria-Gasteiz are obtained from the Meteonorm meteorological database [51]. The hourly ambient temperature is also used to determine the hourly *COP* of HP —obtained for a return temperature of 35 °C [52].

Concerning the heat losses of the TES, these are calculated for both HT and LT levels in [41], according to the procedure developed in the Technical Guide "Design and calculation of the thermal insulation of pipes, appliances and equipment" [53].

Regarding the investment and maintenance costs —shown in Table 3—, data are obtained from the BEDEC database [54] and from the CYPE Construction Price Generator [55]. In the case of ICE, data are obtained from [49]. The ST costs include the solar panels, primary circuit, solar tank and installation [46]; whereas, in the PV installation, the modules and inverters are considered. Apart from this, in order to calculate the annual amortization of the investment, the effective interest rate i has to be known. This value is assumed to be 5% [56,57]. Furthermore, the income of electricity sales for both ICE and PV technologies are 4.58c€/kWh and 5.06c€/kWh, respectively [58].

As shown in Table 3, the investment cost functions of ICE and TES vary according to a potential function, so they have to be approximated to linear functions through line segments. In this linearization, the electric power and volume are divided into different segments for ICE and TES, respectively, obtaining an $a \cdot x + b$ type expression. The coefficients a and b for ICE are those shown in Table 4:

The linearized cost function for ICE is expressed by the following equations:

Table 7
Prices and GHG emissions of resources.

Resource	Price (c€/kWh)	$CO_{2\text{-eq}}$ (g/kWh)
Natural gas	5.73	252
Biomass	5.19	0
Electricity	12.41	399

$$C_{ICE} = 5714.70 \cdot x_1 + 2676.37 \cdot x_2 + 3038.33 \cdot \lambda_2 + 1889.93 \cdot x_3 + 6970.54 \cdot \lambda_3 + 1488.78 \cdot x_4 + 10982.01 \cdot \lambda_4 + 1119.16 \cdot x_5 + 18374.47 \cdot \lambda_5 \quad (86)$$

$$\dot{E}_{ICE,NOM} = x_1 + x_2 + x_3 + x_4 + x_5 \quad (87)$$

$$\lambda_1, \lambda_2, \lambda_3, \lambda_4, \lambda_5 \ bin \quad (88)$$

$$\lambda_1 + \lambda_2 + \lambda_3 + \lambda_4 + \lambda_5 = 1 \quad (89)$$

$$0 \leq x_1 \leq 1 \cdot \lambda_1 \quad (90)$$

$$1 \cdot \lambda_2 \leq x_2 \leq 5 \cdot \lambda_2 \quad (91)$$

$$5 \cdot \lambda_3 \leq x_3 \leq 10 \cdot \lambda_3 \quad (92)$$

$$10 \cdot \lambda_4 \leq x_4 \leq 20 \cdot \lambda_4 \quad (93)$$

$$20 \cdot \lambda_5 \leq x_5 \leq 50 \cdot \lambda_5 \quad (94)$$

In the case of TES, the coefficients are shown in Table 5:

Through applying the linearization by segments, the cost function for TES can be expressed as follows:

$$C_{TES} \geq 3.1635 \cdot x_1 + 1.7601 \cdot x_2 + 701.69 \cdot \lambda_2 + 1.0360 \cdot x_3 + 1358.3 \cdot \lambda_3 - M \cdot (1 - BB) \quad (95)$$

$$V_{TES} = x_1 + x_2 + x_3 \quad (96)$$

$$\lambda_1, \lambda_2, \lambda_3 \ bin \quad (97)$$

$$\lambda_1 + \lambda_2 + \lambda_3 = 1 \quad (98)$$

$$0 \leq x_1 \leq 500 \cdot \lambda_1 \quad (99)$$

$$500 \cdot \lambda_2 \leq x_2 \leq 1000 \cdot \lambda_2 \quad (100)$$

$$1000 \cdot \lambda_3 \leq x_3 \leq V_{max} \cdot \lambda_3 \quad (101)$$

Besides the economic data of technologies, the environmental impact also has to be known. The GHG emitted during the manufacture of devices are expressed through regression equations obtained using both the Ecoinvent 3 [59] and the BEDEC [54] databases. This information is shown in Table 6.

On the other hand, both the price and environmental impact [60] of the energy resources are also determined. These prices and emissions —outlined in Table 7— correspond to the economic and environmental values in the construction period. The aim of considering the prices and emissions in this period is to compare the optimal solutions with the current installation, whose technical, economic and environmental feasibilities were analysed under those conditions. In the case of environmental impact of biomass, in the construction period it was considered carbon–neutral and no GHG emissions of its preparation and transport were considered.

2.4.2. Legal constraints

As aforementioned, the feasibility of the plant is closely related to the normative in force in the country where the building is located. For this reason, legal constraints have to be analysed for the case study.

In this case, the CTE determines that a certain percentage of the DHW demand must be supplied by renewable energy sources or high efficiency systems, such as cogeneration [42]. Thus, the sum of thermal energy production by the ICE, the BB and the ST_{HT} has to be equal to or greater than the minimum renewable —or high efficiency— contribution (RC_{min}) required, which is variable depending on the climate zone.

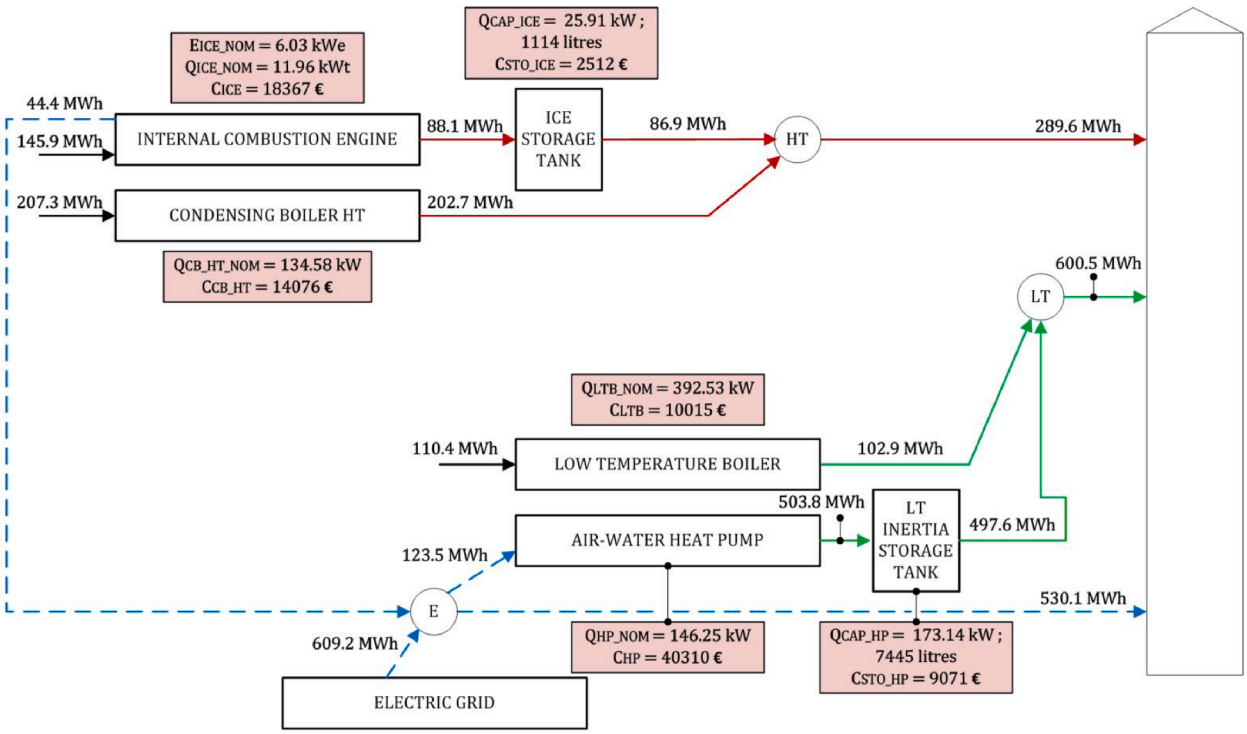

Fig. 5. Economic optimal configuration.

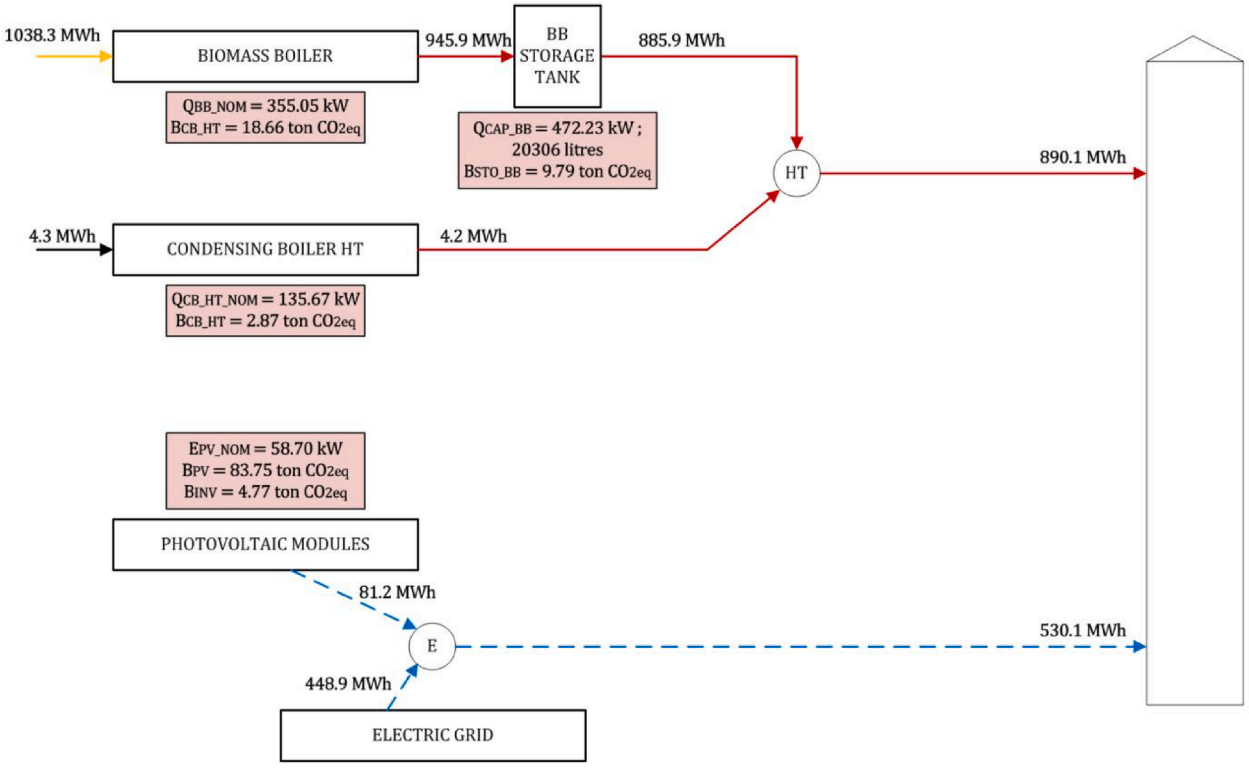

Fig. 6. Optimal environmental configuration.

$$\sum_{h}\left(Q_{STO,ICE}(d,h)+Q_{STO,BB}(d,h)+Q_{ST,HT}(d,h)\right) \geq RC_{min}\cdot\sum_{d}\sum_{h}Q_{DHW}(d,h) \quad (102)$$

Moreover, the CTE requires that solar energy installations include a conventionally fuelled auxiliary system, which ensures the continuation of supply. The sizing of this auxiliary system is carried out considering that all the demand can be covered by the auxiliary system [61]—as if solar thermal were not installed. The auxiliary system will only start up when the energy generated by the collectors is not enough to supply the energy demand. CB and LTB are the technologies conventionally used as auxiliary systems [62]; whereas BB, ICE and HP are technologies used as auxiliary systems or as an alternative to ST. Apart of this, according to the CTE, if solar thermal is installed, the ratio between the solar tank volume and the solar collector surface $r_{V\text{-}S}$ must be in the interval 50 – 180 L/m^2 (Eq. (67).

When the auxiliary system is used to supply HT demand, the sum of the nominal thermal power of all the conventional technologies operating at HT has to be greater than the maximum demand at HT —DHW demand and heating demand when this is supplied at this temperature level ($HEAT_{HT}=1$).

$$\dot{Q}_{CB\_HT\_NOM}+\dot{Q}_{BB\_NOM}\geq\dot{Q}_{DHW,MAX}+\dot{Q}_{HEAT,MAX}\bullet HEAT_{HT} \quad (103)$$

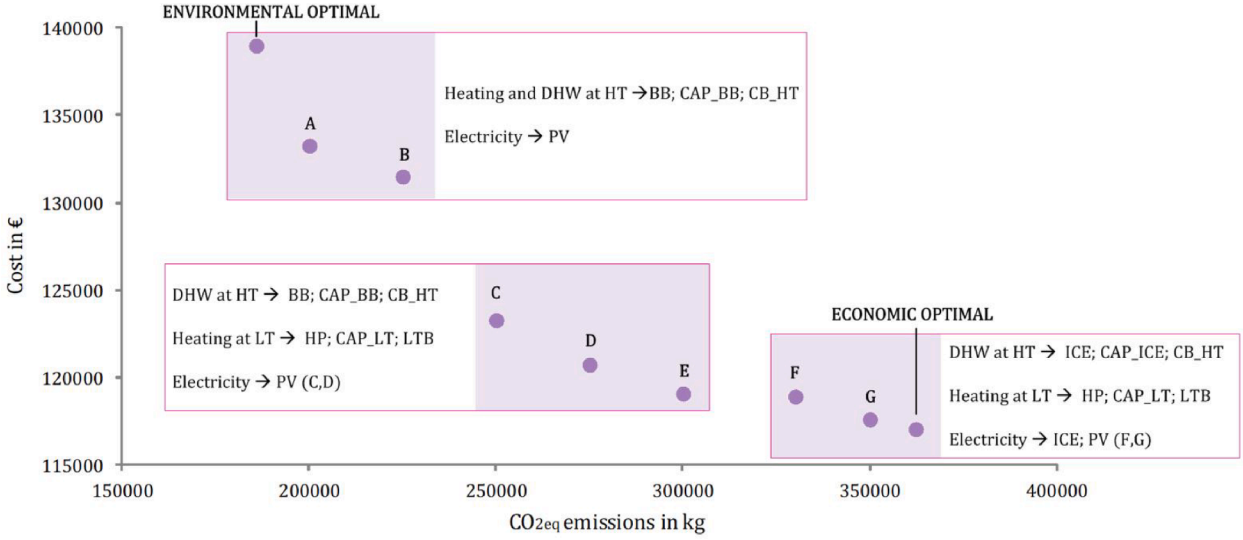

Fig. 7. Pareto Front of the case study.

Table 8
Optimal solutions of the Pareto Front.

		Unit	Env. optimal	A	B	C	D	E	F	G	Econ. optimal
BB	Q_{BB_NOM}	kW	355.1	228.0	195.6	59.8	54.9	41.4	–	–	–
BB STO	V_{BB}	l	20,306	17,465	15,160	6024	5119	3479	–	–	–
ICE	E_{ICE_NOM}	kW	–	–	–	–	–	–	6.2	6.2	6.0
ICE STO	V_{ICE}	l	–	–	–	–	–	–	1137	966	1114
CB_HT	$Q_{CB\_HT\_NOM}$	kW	135.7	231.3	270.4	74.8	79.7	93.2	134.6	134.6	134.6
ST	S_{ST}	kW	–	–	–	–	–	–	–	–	–
ST STO	V_{VST}	l	–	–	–	–	–	–	–	–	–
CB_LT	$Q_{CB\_LT\_NOM}$	kW	–	–	–	–	–	–	–	–	–
LTB	Q_{LTB_NOM}	kW	–	–	–	338.8	371.1	382.2	371.1	371.1	392.5
HP	Q_{HP_NOM}	kW	–	–	–	200.0	167.7	156.6	167.7	167.7	146.3
LT STO	V_{LT}	l	–	–	–	16,985	9239	8747	9239	9239	7445
PV	E_{PV_NOM}	kW	58.7	58.7	28.1	58.7	28.8	–	53.8	14.7	–
Consumed biomass		MWh/a	1038.3	922.6	882.3	327.7	306.2	268.2	–	–	–
Consumed NG-total		MWh/a	4.3	62.5	102.5	31.6	91.3	140.7	432.5	434.1	463.6
Consumed NG-ICE		MWh/a	–	–	–	–	–	–	152.5	145.7	145.9
Useful heat-ICE		MWh/a	–	–	–	–	–	–	90.7	86.9	86.9
Produced electricity-ICE		MWh/a	–	–	–	–	–	–	46.4	44.3	44.4
Produced electricity-PV		MWh/a	81.2	81.2	38.9	81.2	39.9	–	74.5	20.3	–
Consumed electricity- HP		MWh/a	–	–	–	143.2	132.0	128.3	132.0	130.8	123.5
Purchased electricity		MWh/a	448.9	448.9	491.2	592.1	622.2	658.4	541.2	596.3	609.2
Sold electricity		MWh/a	0	0	0	0	0	0	0	0	0
REE		%	–	–	–	–	–	–	89.71	90.14	89.98
PES		%	–	–	–	–	–	–	25.20	25.28	25.26
Annual amortization		€/a	21,625	19,285	13,424	21,524	14,848	9288	18,053	11,429	8246
O&M cost		€/a	117,361	113,978	118,072	101,764	105,895	109,799	100,874	106,188	108,505
Annual overall cost		€/a	138,986	133,263	131,496	123,288	120,743	119,087	118,927	117,617	116,751
$CO_{2\text{-eq}}$ of components		Ton/a	5.6	5.2	3.2	5.9	3.7	1.9	5.1	2.7	1.8
Operation $CO_{2\text{-eq}}$		Ton/a	180.2	194.8	221.8	244.1	271.3	298.1	324.9	347.3	359.9
Annual overall $CO_{2\text{-eq}}$		Ton/a	185.8	200.0	225.0	250.0	275.0	300.0	330.0	350.0	361.7

In the case of LT terminal units, the sum of the nominal thermal power of all the conventional technologies that operate at LT has to be greater than the maximum demand at LT ($HEAT_{HT} = 0$).

$$\dot{Q}_{CB\_LT\_NOM} + \dot{Q}_{LTB\_NOM} + \dot{Q}_{HT\_NOM} \geq \dot{Q}_{HEAT,MAX} \cdot (1 - HEAT_{HT}) \quad (104)$$

With respect to cogeneration, the EED [39] establishes that micro-CHP can be considered as high efficiency cogeneration whenever primary energy savings (PES) are achieved compared to the separate production of heat and electricity through conventional means. Hence, the PES indicator has to be positive.

$$PES(\%) = \left(1 - \frac{1}{\frac{\eta_Q}{Ref\,H_\eta} + \frac{\eta_E}{Ref\,E_\eta}}\right) \cdot 100 \geq 0 \quad (105)$$

where η_E and η_Q are the average electric and thermal efficiencies of the cogeneration system, and $Ref\ E_\eta$ and $Ref\ H_\eta$ are the harmonised reference values for the separate production of electricity and heat established by the European Commission in application of Directive 2012/27/EU [63]. The harmonised reference efficiency of the separate production of electricity corresponds to the overall efficiency of the electric grid –including grid losses–, whereas the harmonised value of the separate production of heat is the efficiency of generating it through a natural gas boiler. According to Directive 2012/27/EU, for natural gas fuelled cogeneration installations projected before 2016, the harmonised reference efficiencies for the separate production of electricity and heat are 45% and 90%, respectively.

If a buffer tank is installed with the cogeneration unit, the useful heat

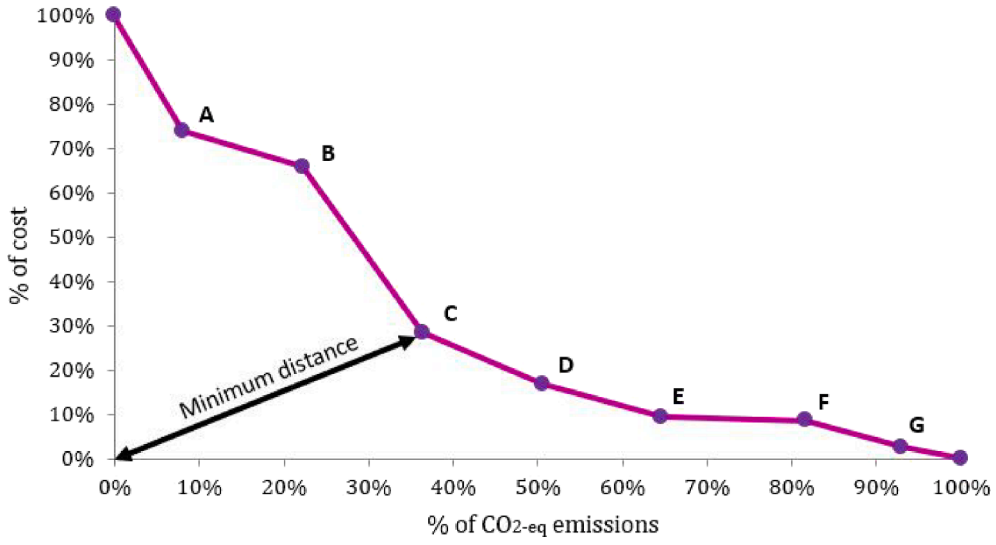

Fig. 8. Multi-objective solution in percentage terms.

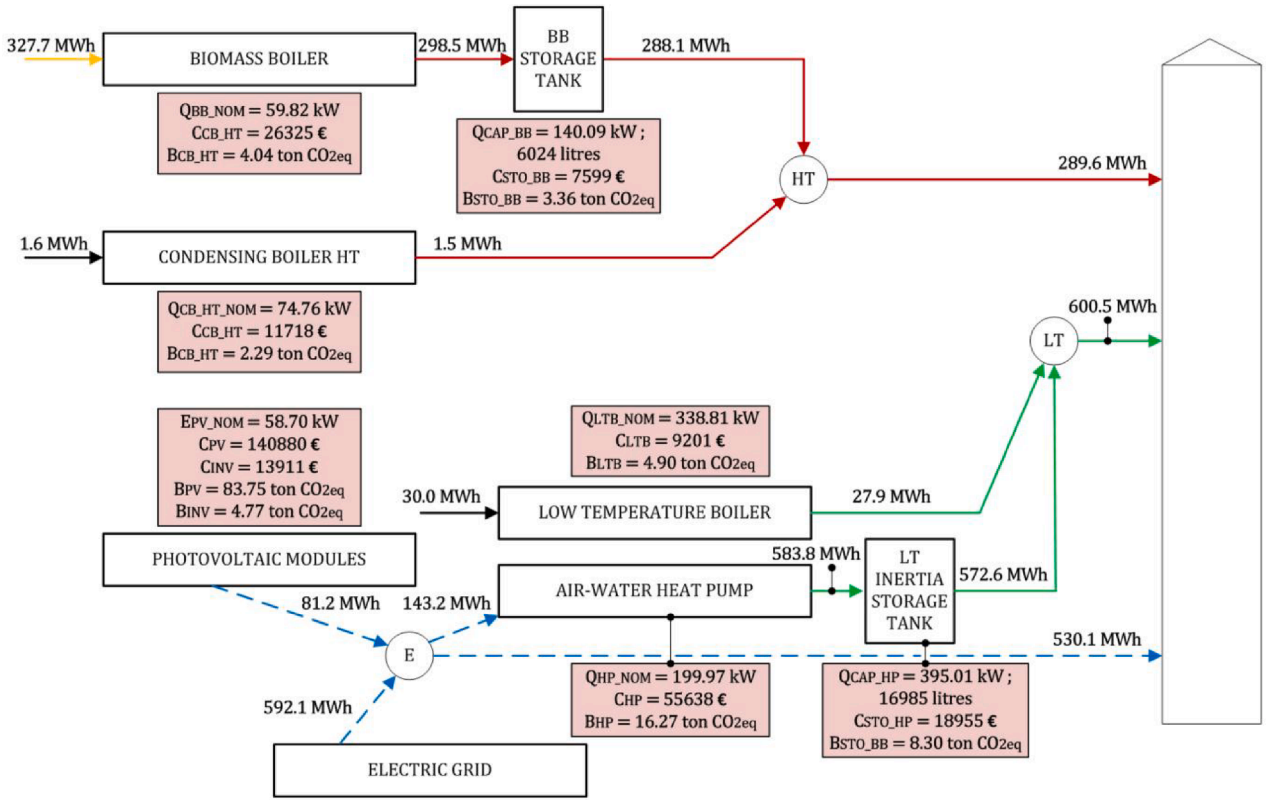

Fig. 9. Optimal multi-criteria configuration.

obtained from the TES has to be considered for calculating thermal efficiency, instead of the gross heat produced by the engine. Furthermore, the PES indicator has to be greater than zero only if the micro-CHP unit is installed. According to these considerations, the constraint is expressed as:

$$\frac{\sum_d \sum_h Q_{STO,ICE}(d,h) / \sum_d \sum_h F_{ICE}(d,h)}{Ref H_\eta} + \frac{\sum_d \sum_h E_{ICE}(d,h) / \sum_d \sum_h F_{ICE}(d,h)}{Ref E_\eta} - 1 + M(1 - ICE) \geq 0 \tag{106}$$

The same criterion is considered for the equivalent electric efficiency (REE) indicator. The Spanish Royal Decree 661/2007 [64] determines the cogeneration efficiency by means of the REE, which compares the cogenerated electricity and the conventional electricity production. This Royal Decree establishes that the REE must be greater than or equal to 49.5% in the case of natural gas micro-CHP engines.

$$REE = \frac{E_{ICE}}{F_{ICE} - \left(\frac{Q_{ICE,U}}{Ref H_\eta}\right)} \geq 49.5\% \tag{107}$$

The minimum value of the REE of the micro-CHP, as is the case with the PES, is only considered when this technology is installed ($ICE = 1$):

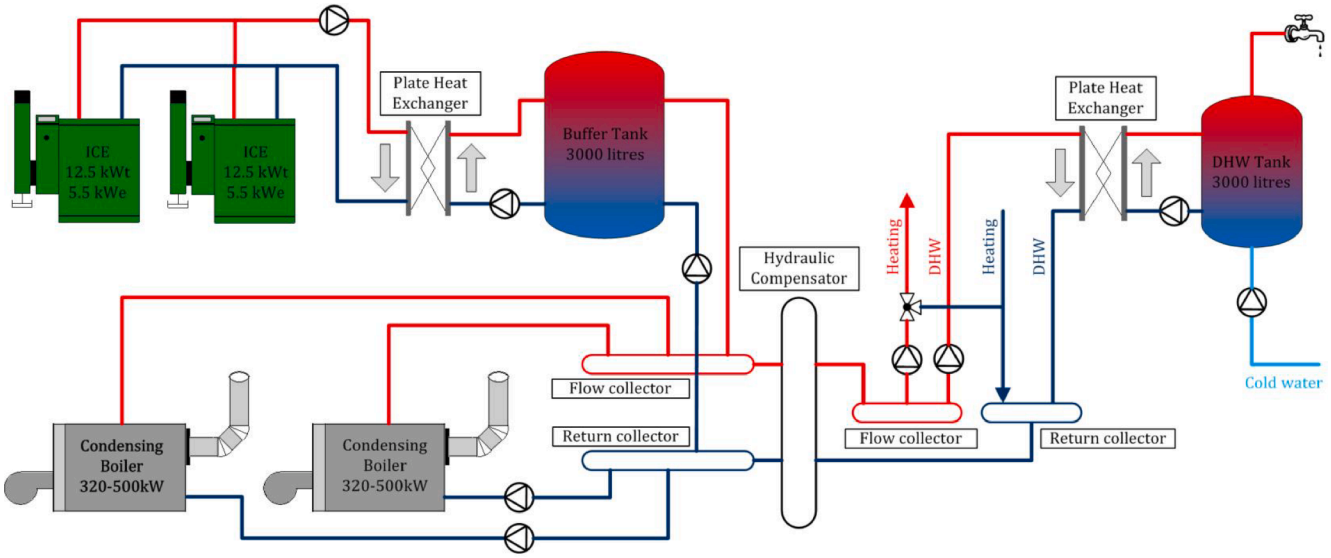

Fig. 10. Hydraulic scheme of the current thermal plant.

$$\sum_d \sum_h E_{ICE}(d,h) \geq 0.495 \cdot \left(\sum_d \sum_h F_{ICE}(d,h) - \sum_d \sum_h Q_{STO,ICE}(d,h) \Big/ RefH_\eta \right) - M \cdot (1 - ICE) \quad (108)$$

3. Results and discussion

3.1. Optimal economic configuration

The optimal structure of the plant which minimizes the overall economic cost is shown in Fig. 5. The optimal nominal power and the investment cost of each technology, as well as the annual energy streams, are depicted. The DHW demand is supplied by an ICE with a nominal electric power of 6.03 kWe and a nominal thermal power of 11.96 kWt, supported by a natural gas condensing boiler. In the optimal heating system, LT terminal units are installed and this demand is supplied by an air–water heat pump supported by a low temperature boiler. Both the heat pump and users' electricity consumption are supplied by the ICE and the electricity grid.

3.2. Optimal environmental configuration

The optimal environmental structure, which minimizes the equivalent CO_2 emissions, is made of both a biomass boiler and a condensing boiler to supply all the thermal demand at HT, as shown in Fig. 6. Most of the thermal energy is provided by the biomass boiler, whereas the condensation boiler is only used for peak demand periods. Since the TES capacity for the biomass boiler and the volume of wood pellet storage require a large additional space, a technical feasibility study should be carried out to determine if the proposal can be implemented.

Regarding the electricity demand, this is supplied by both PV modules and electricity from the grid, the installed surface of PV modules being the maximum surface supposed for this technology.

3.3. Optimal multi-criteria configuration

The first step for defining the Pareto front is to establish the upper and lower limits of the f1 function —where CO_2-eq emissions are minimized—, and whose values correspond to the optimal economic (361.7 ton of CO_2-eq) and environmental (185.8 ton of CO_2-eq) configurations, respectively. The interval between these values is divided into 8 subintervals, obtaining A-G points with their respective values of ε_j (ε_A, ε_B, …, ε_G). In Fig. 7, the solutions of the Pareto Front are outlined.

At points A and B —which are the closest to the environmental optimum—, the structure is composed of a biomass boiler and an auxiliary condensing boiler to supply DHW and heating at HT. Both cases include PV modules for electricity generation. According to the results outlined in Table 8, as CO_2-eq emissions increase and the global cost decreases, the PV surface is reduced, as well as the biomass boiler's nominal power, whereas the nominal power of the condensing boiler is greater.

In the optimal configuration for the points C, D and E, heating is generated at LT with air source heat pumps supported by low temperature boilers. To supply DHW, a biomass boiler is installed with a condensing boiler as support for peak demand periods. PV modules are installed in both cases C and D, reducing the installed nominal power

Table 9
Comparative analysis among the optimal solutions and the current installation.

		Unit	Environm. optimal	Multiobjc. optimal	Economic optimal	Current installation
BB	Q_{BB_NOM}	kW	355.1	59.8	–	–
BB STO	V_{BB}	l	20,306	6024	–	–
ICE	E_{ICE_NOM}	kW	–	–	6.0	11.0
ICE STO	V_{ICE}	l	–	–	2512	3000 (+3000)
CB_HT	$Q_{CB\_HT\_NOM}$	kW	135.7	74.8	134.6	1000
ST	S_{ST}	kW	–	–	–	–
ST STO	V_{VST}	l	–	–	–	–
CB_LT	$Q_{CB\_LT\_NOM}$	kW	–	–	–	–
LTB	Q_{LTB_NOM}	kW	–	338.8	392.5	–
HP	Q_{HP_NOM}	kW	–	200.0	146.3	–
LT STO	V_{LT}	l	–	16,985	9071	–
PV	E_{PV_NOM}	kW	58.7	58.7	–	58.7
Consumed biomass		MWh/a	1038.3	327.7	–	–
Consumed NG-total		MWh/a	4.3	31.6	463.6	1086.5
Consumed NG-ICE		MWh/a	–	–	145.9	327.5
Useful heat-ICE		MWh/a	–	–	86.9	195.5
Produced electricity-ICE		MWh/a	–	–	44.4	87.9
Produced electricity-PV		MWh/a	81.2	81.2	–	81.2
Consumed electricity- HP		MWh/a	–	143.2	123.5	–
Purchased electricity		MWh/a	448.9	592.1	609.2	361.0
Sold electricity		MWh/a	0	0	0	0
REE		%	–	–	89.98	79.71
PES		%	–	–	25.26	20.60
Annual amortization		€/a	21,625	21,524	8246	20,857
O&M cost		€/a	117,361	101,764	108,505	113,370
Annual overall cost		€/a	138,986	123,288	116,751	134,227
$CO_{2\text{-eq}}$ of components		Ton/a	5.6	5.9	1.8	4.9
Operation $CO_{2\text{-eq}}$		Ton/a	180.2	244.1	359.9	417.9
Annual overall $CO_{2\text{-eq}}$		Ton/a	185.8	250.0	361.7	422.8

Table 10
Electricity tariffs.

Tariff		0–1 h	1–7 h	7–12 h	12–13 h	13–22 h	22–23 h	23–24 h
No hourly discrimination (NHD)		0.1241	0.1241	0.1241	0.1241	0.1241	0.1241	0.1241
2-period hourly discrimination (2PHD)	Summer	0.0580	0.0580	0.0580	0.0580	0.1488	0.1488	0.0580
	Winter	0.0580	0.0580	0.0580	0.1488	0.1488	0.0580	0.0580

Table 11
Influence of electricity tariffs.

		Unit	**Econ. optimal**	2PHD
BB	Q_{BB_NOM}	kW	**–**	–
BB STO	V_{BB}	l	**–**	–
ICE	E_{ICE_NOM}	kW	**6.0**	17.0
ICE STO	V_{ICE}	l	**1114**	3451
CB_HT	$Q_{CB\_HT\_NOM}$	kW	**134.6**	134.6
ST	S_{ST}	kW	**–**	–
ST STO	V_{VST}	l	**–**	–
CB_LT	$Q_{CB\_LT\_NOM}$	kW	**–**	–
LTB	Q_{LTB_NOM}	kW	**392.5**	345.0
HP	Q_{HP_NOM}	kW	**146.3**	193.8
LT STO	V_{LT}	l	**7445**	15,152
PV	E_{PV_NOM}	kW	**–**	–
Consumed biomass		MWh/a	**–**	–
Consumed NG-total		MWh/a	**463.6**	395.8
Consumed NG-ICE		MWh/a	**145.9**	150.7
Useful heat-ICE		MWh/a	**86.9**	86.9
Produced electricity-ICE		MWh/a	**44.4**	45.8
Produced electricity-PV		MWh/a	**–**	–
Consumed electricity- HP		MWh/a	**123.5**	142.3
Purchased electricity		MWh/a	**609.2**	626.6
Sold electricity		MWh/a	**0**	0
REE		%	**89.98**	84.59
PES		%	**25.26**	24.02
Annual amortization		€/a	**8246**	11,636
O&M cost		€/a	**108,505**	93,030
Annual overall cost		€/a	**116,751**	104,666
$CO_{2\text{-eq}}$ of components		Ton/a	**1.8**	2.3
Operation $CO_{2\text{-eq}}$		Ton/a	**359.9**	349.8
Annual overall $CO_{2\text{-eq}}$		Ton/a	**361.7**	352.1

until case E, when its installation becomes economically unprofitable.

Finally, cases F and G have the same configuration for the economic optimum, with the exception of the installation of PV modules, whose surface decreases as the global cost gets lower; and finally they are not installed in the economic optimum. Hence, DHW is produced by ICE-based micro-CHP and condensing boiler technologies; while space heating is generated at LT by an air–water heat pump with low temperature boiler as the auxiliary system. The micro-CHP engine —as well as the PV modules in cases F and G— provides electricity to meet both the end-user demand and the heat pump consumption.

The solution for the multi-objective problem is the point of the Pareto Front which achieves greater improvements in percentage terms when both objectives are considered at the same time. Therefore, as shown in Fig. 8, point C of the Pareto Front is the optimal multi-objective solution as it is the closest to the origin of the objective-axes.

In Fig. 9, the optimal structure of point C is illustrated. As can be seen, a biomass boiler would provide most of the DHW demand and peak demands would be covered by the condensing boiler. Meanwhile, the air-source heat pump technology —partially fuelled by PV modules— is used to supply heating at low temperature, supported by a low temperature boiler.

3.4. Validation

In order to validate the proposed method, the results are compared with those obtained for the current installation operating under optimal conditions. The current installation has two natural gas-fuelled micro-cogeneration units —based on reciprocating internal combustion engines—, supported by two natural gas-fired condensing boilers. Besides that, the residential building includes PV modules integrated in the facade.

The centralized heating and DHW installation produces hot water at 80°/60 °C. It is composed of two natural gas condensing boilers that operate in cascade with a modulation range of 320–500 kW. As mentioned above, the CTE establishes a minimum contribution of renewable energy sources or high efficiency systems to the DHW production. This value is 30% for the location of the building under study. For that purpose, two ICE-based micro-CHP units are installed with TES arranged in parallel. These engines operate at full load —with no modulation possibility— and the thermal and electric nominal power of each unit are 12.5 kW and 5.5 kW, respectively. Apart from this, they are

Table 12
Influence of market prices.

			Electricity −30%			**Electricity 0%**			Electricity 30%		
		Unit	NG −30%	NG 0%	NG 30%	NG −30%	**NG 0%**	NG 30%	NG −30%	NG 0%	NG 30%
BB	Q_{BB_NOM}	kW	–	16.0	52.8	–	**–**	51.0	–	–	52.9
BB STO	V_{BB}	l	–	681	4828	–	**–**	4700	–	–	4852
ICE	E_{ICE_NOM}	kW	10.0	–	–	29.1	**6.0**	–	45.6	29.9	–
ICE STO	V_{ICE}	l	853	–	–	8007	**1114**	–	10,830	7855	–
CB_HT	$Q_{CB\_HT\_NOM}$	kW	134.6	118.7	81.8	421.7	**134.6**	83.6	373.4	134.6	81.7
ST	S_{ST}	kW	–	–	–	–	**–**	–	–	–	–
ST STO	V_{VST}	l	–	–	–	–	**–**	–	–	–	–
CB_LT	$Q_{CB\_LT\_NOM}$	kW	–	–	–	–	**–**	–	–	–	–
LTB	Q_{LTB_NOM}	kW	406.5	372.5	343.0	–	**392.5**	355.2	–	411.0	378.7
HP	Q_{HP_NOM}	kW	132.3	166.3	195.8	–	**146.3**	183.5	–	127.7	160.1
LT STO	V_{LT}	l	6557	9198	15,759	–	**7445**	12,286	–	7260	9198
PV	E_{PV_NOM}	kW	–	–	–	–	**–**	–	–	58.7	58.7
Consumed biomass		MWh/a	–	113.3	300.3	–	**–**	298.5	–	–	301.7
Consumed NG-total		MWh/a	505.5	269.9	55.4	1165.9	**463.6**	74.5	1364.4	642.6	104.3
Consumed NG-ICE		MWh/a	179.9	–	–	642.3	**145.9**	–	988.0	484.3	–
Useful heat-ICE		MWh/a	106.4	–	–	378.0	**86.9**	–	521.9	277.9	–
Produced electricity-ICE		MWh/a	54.7	–	–	195.3	**44.4**	–	300.3	147.3	–
Produced electricity-PV		MWh/a	–	–	–	–	**–**	–	–	81.2	81.2
Consumed electricity- HP		MWh/a	116.9	131.5	142.0	–	**123.5**	137.8	–	114.5	129.6
Purchased electricity		MWh/a	592.3	661.6	672.1	342.0	**609.2**	667.9	267.6	416.5	578.5
Sold electricity		MWh/a	0	0	0	7.2	**0**	0	37.8	0.4	0
REE		%	88.69	–	–	87.85	**89.98**	–	73.58	83.92	–
PES		%	24.97	–	–	24.79	**25.26**	–	20.78	23.87	–
Annual amortization		€/a	8423	8860	11,137	7344	**8246**	10,486	8689	20,908	19,670
O&M cost		€/a	78,099	84,935	85,106	96,826	**108,505**	110,652	106,443	115,356	125,340
Annual overall cost		€/a	86,522	93,795	96,243	104,170	**116,751**	121,138	115,132	136,264	145,010
$CO_{2\text{-eq}}$ of components		Ton/a	1.7	1.7	2.2	1.2	**1.8**	2.1	1.5	5.8	5.5
Operation $CO_{2\text{-eq}}$		Ton/a	363.7	332.0	282.1	430.3	**359.9**	285.3	450.6	328.1	257.1
Annual overall $CO_{2\text{-eq}}$		Ton/a	365.4	333.7	284.4	431.5	**361.7**	287.4	452.1	333.9	262.6

Table A1
Characteristics of dwelling models.

DWELLING TYPE	T1	T2	T3	T4	T5	T6	T7	T8	T9	T10	T11	T12	T13	T14	T15	T16
Useful surface (m^2)	82	60	61	47	60	48	49	68	87	87	53	85	83	44	69	79
Number of dwellings	8	16	16	16	16	8	8	8	8	16	16	8	8	8	8	8
Bedrooms (u)	2	2	2	1	2	1	1	2	3	3	2	3	2	1	2	3
Bathrooms and toilets (u)	1	1	1	1	1	1	1	1	2	2	1	2	1	1	1	2

Table A2
Characteristics of thermal zones.

	Dwellings	Useful surface (m^2)
PV1 (P2-P7)	T1-T2-T3-T4-T5	338.94
PV2	T6-T7-T8	217.36
PV3A	T9-T10-T11	269.07
PV3B	T10-T11-T12	263.46
PV4	T13-T14-T15	239.54
PV5	T2-T3-T4-T5-T16	337.74

directly connected to a buffer tank —which has a capacity of 3000 L— through a plate heat exchanger. This configuration allows simultaneous charging and discharging. The heat is distributed to both space heating terminal units and a DHW tank of 3000 L through a flow collector. The hydraulic scheme is shown in Fig. 10.

Moreover, 256 PV modules are mounted over a structure installed on the south façade —as shown in Fig. 3 and —, having an inclination of 60°. The peak power installed is 58,688 W_p. In order to transform the direct current generated by the panels to alternating current, 12 inverters of 5 kW each are installed.

3.4.1. Optimal operation of the current installation

The operation strategy of the current installation has been optimized according to both economic and environmental aspects. The optimization models are those explained in Section 2, while also fixing both the configuration and the capacity of the devices. Since only the operation is optimized in the current plant, there are no conflicting objectives. Hence, the optimal operation strategy is the same for both objectives, where micro-CHP units operate to meet the thermal energy demand and guarantee an efficient use of the energy resources, so their functioning has preference over the condensation boiler.

In Table 9, energy, economic and environmental results are summarized to compare the economic, environmental and multi-criteria optimizations with the current installation. The optimal economic and multi-criteria solutions get better results, both economic and environmental, compared to the real plant, principally due to the decrease in operation costs and emissions. The investment cost is greater in the optimal multi-criteria solution than in the economic one —owing to the installation of PV modules—; whereas the operation cost is lower. Regarding the emissions of GHG, these are reduced from 14.5% in the economic optimum to 56.1% in the environmental optimum. As shown, emissions associated with the manufacturing of the equipment —which are greater in solutions with PV modules— contribute to the overall environmental impact in less than 3% in all cases.

3.5. Sensitivity analysis

The optimization of energy systems is susceptible to any modification in the energy market and therefore requires a sensitivity analysis to determine the dependence of the system on the different external factors involved. In this section, a sensitivity analysis has been carried out, taking into consideration the hourly discrimination in the electricity tariff and the variation in both electricity and natural gas prices.

Regarding the electricity tariffs, the ones with hourly discrimination achieve better demand management, rewarding users who consume electricity during off-peak hours or self-consume the electricity generated during peak hours. In order to assess the influence of electricity

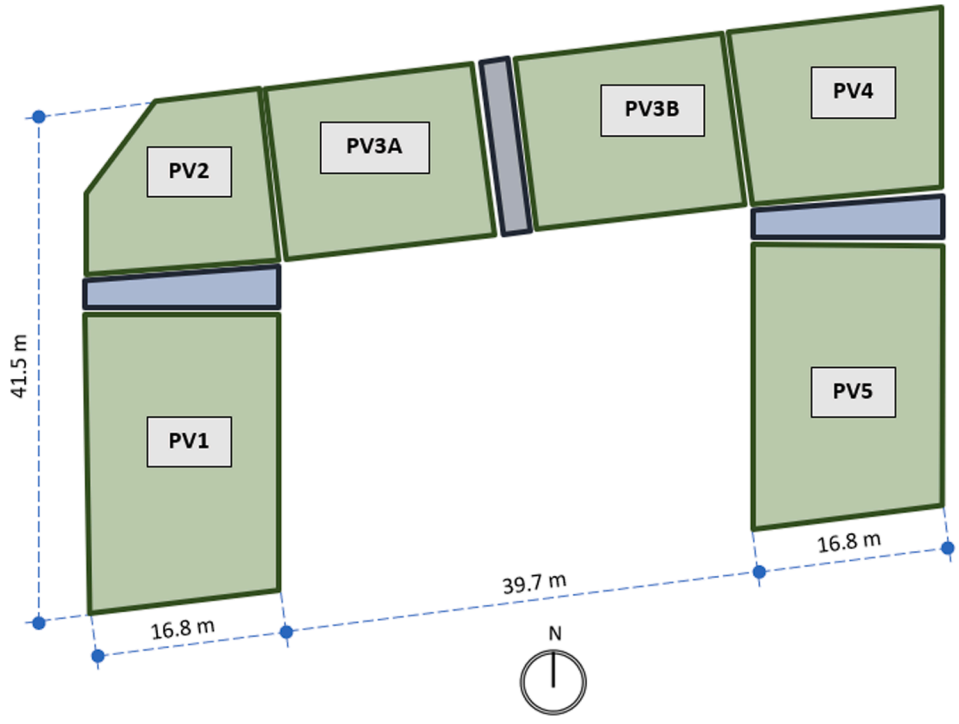

Fig. A1. Floor plan of the building under study.

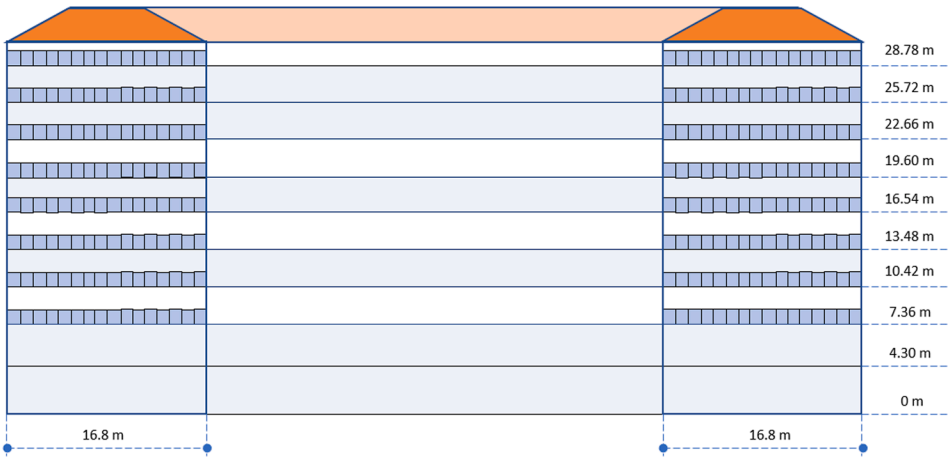

Fig. A2. Plan of the south façade.

Table A3
Thermal transmittances of enclosures and partitions.

	U-value [W/(m^2·K)]
Precast concrete façade	0.331
Partition between common areas and dwellings	0.276
Roof	0.399
Floor	0.230

Table A4
Minimum required ventilation rate.

	Min. required ventilation rate [l/s]		
	Per person	*Per m^2*	*Other parameters*
Bedroom	5		
Living room	3		
Bathroom and Toilet			15 per room
Kitchen		2	
Junk rooms and common areas		0.7	

price variation, a new scenario is proposed —a 2-period hourly discrimination tariff (2PHD)—; it is then compared to the optimal economic solution for which no hourly discrimination tariff is assumed. As mentioned above, this electricity tariff, summarized in Table 10, corresponds to the electricity prices in the construction year [65].

As shown in Table 11, the lowest overall cost is obtained for the two-period tariff, for which the configuration of the plant is the same as that obtained for the optimal economic reference case. Differences are found in larger engine sizes, heat pump and thermal energy storage systems for tariffs with hourly discrimination, including the consequent reduction in the REE and PES. This is due to the fact that, in this last case, the engine operates according to the electricity market prices. Thus, the engine operates during peak hours, providing electricity to both users and heat pump, remaining off during off-peak hours.

Furthermore, a sensitivity analysis has been carried out to determine how both the design and operation strategy vary when a variation of ± 30% is applied to market prices for natural gas and electricity. The obtained solutions are summarized in Table 12. According to these results, micro-CHP technology is found to be less profitable if the price of electricity decreases and the natural gas price increases. By increasing the price of natural gas by 30%, the micro-CHP ceases to be competitive and, as no variation of biomass price is assumed, the biomass boiler supported by natural gas condensing boilers is the most interesting configuration. On the contrary, when the cost of natural gas is reduced by 30% and, for the current electricity cost or higher, the generation of high temperature heating by micro-CHP engines remains the most profitable technology.

If the REE is analysed in micro-CHP solutions, this decreases with the increase in the cost of electricity, which is due to the increase in motor size. By installing greater power capacity and operating at full load, the number of operating hours of the equipment decreases and the losses in the tank increase in percentage terms, since the heat is not used at the moment it is generated or immediately after.

Furthermore, the installed power capacity sizing of the air–water

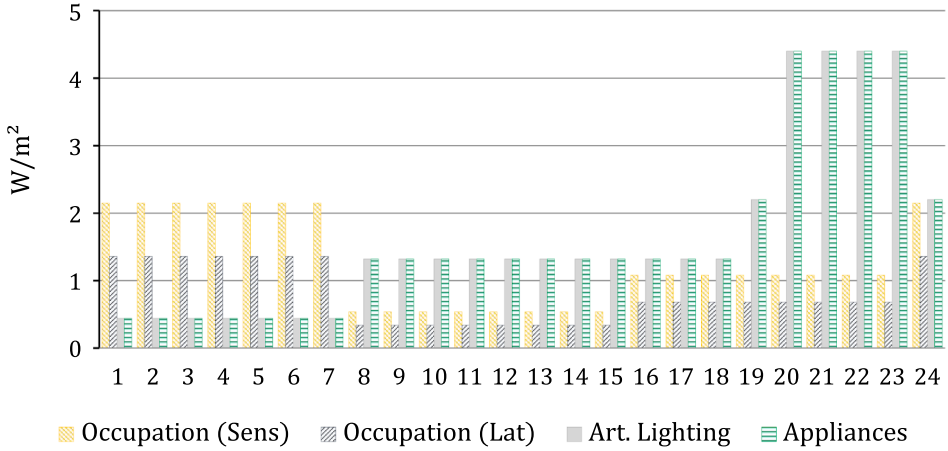

Fig. A3. Hourly profile of internal gains (working days).

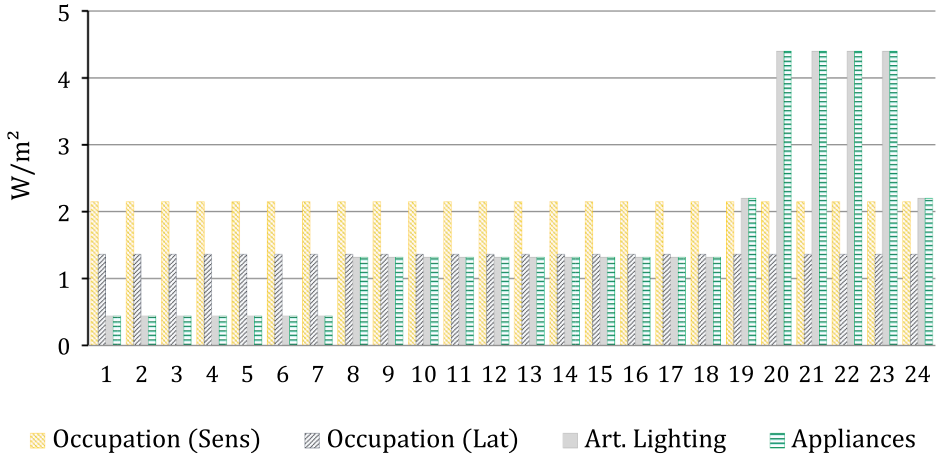

Fig. A4. Hourly profile of internal gains (weekends and holidays).

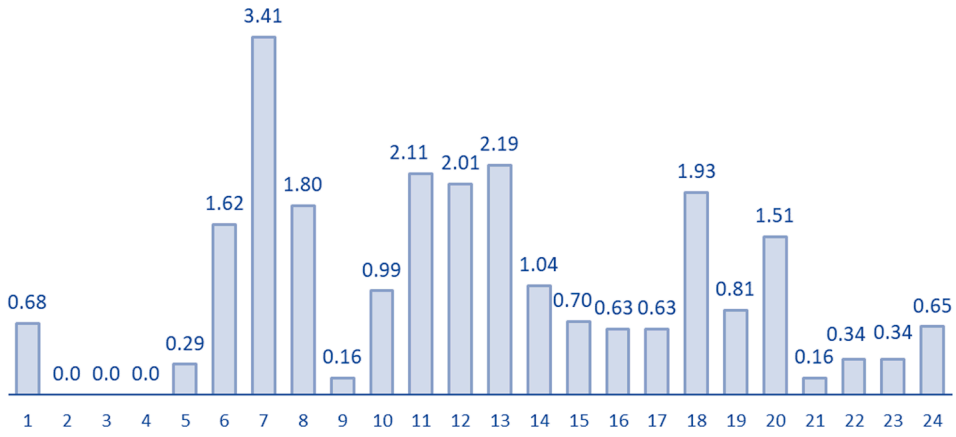

Fig. A5. Hourly multiplicator factors of DHW demand.

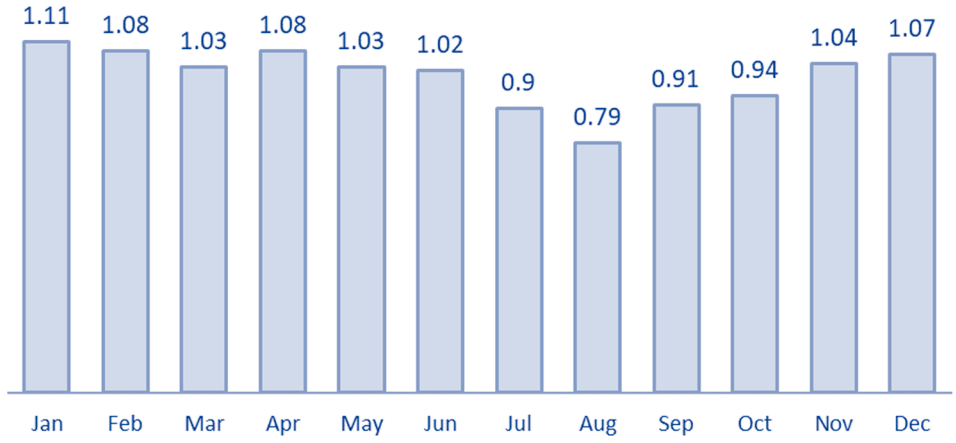

Fig. A6. Monthly multiplicator factors of DHW demand.

heat pump can also be affected by the variation in the purchase prices of electricity and natural gas. A decrease in the price of electricity leads to an increase in installed power capacity, as well as an increase in the cost of natural gas, which makes the air–water heat pump a more suitable solution than natural gas low-temperature boilers.

Regarding the installation of photovoltaic solar technology, it should only be considered when the price of electricity increases and the cost of natural gas is greater than or equal to the current one.

Finally, the sale of electricity can be economically interesting if there is a decrease in the price of natural gas for the current cost of electricity or higher. In this case, the heat pump installation is not a feasible solution and the installed nominal power of the micro-CHP device increases, reducing the overall electricity demand. Indeed, a continuous functioning of the micro-CHP unit at higher power is more profitable, as it enables greater self-consumption, despite selling the surplus electricity at a non-competitive sale price. On the contrary, if the price of

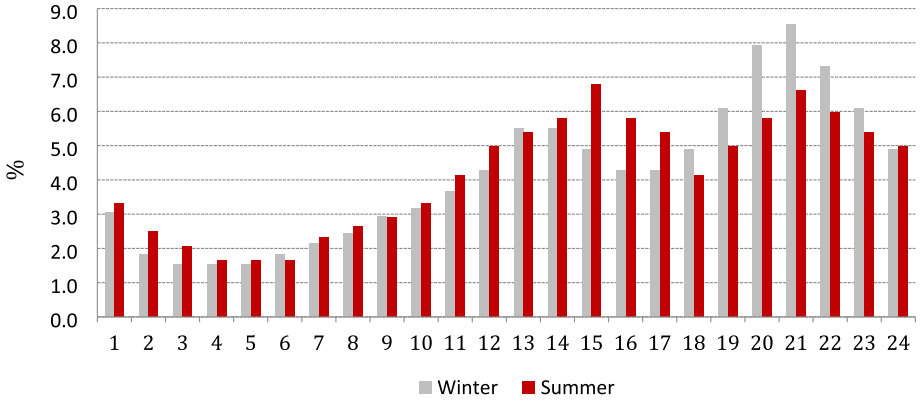

Fig. A7. Daily electricity demand profile in percentage.

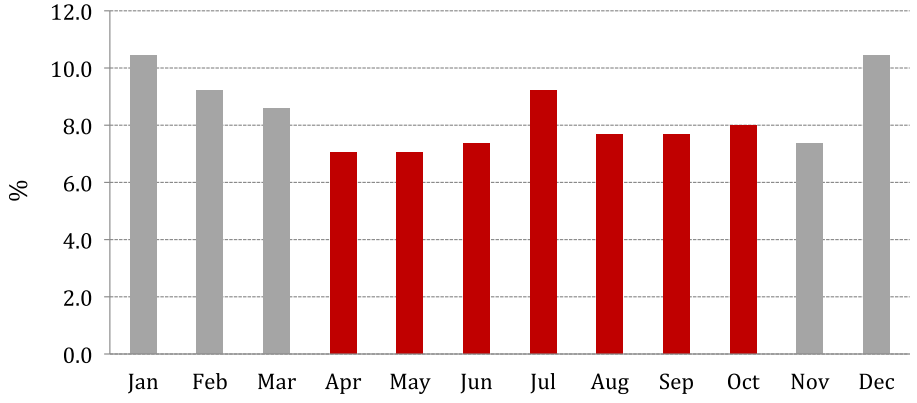

Fig. A8. Annual electricity demand profile in percentage.

electricity rises and the price of natural gas remains constant, the electricity consumption increases due to the use of the heat pump and there is no surplus electricity for the sale.

3.6. Discussion

According to the results, it is demonstrated that the proposed method allows the optimal design and sizing of thermal installations to be determined in the project phase, obtaining better results than those calculated by means of rough methods. The proposed model provides simplicity, reproducibility and flexibility and can be easily adapted to the characteristics of the building, to different technologies and to the current regulations of the country in which the building under study is located. Apart of this, OpenSolver, which is an open-source CBC (COIN-OR Branch-and-Cut) solver, can be easily implemented in widespread software as Excel VBA or Apache OpenOffice, which code is well-known, without additional costs.

Regarding the optimization model, this includes 7176 operation-variables (23 variables · 13 representative days · 24 h), 55 sizing-variables and 13,505 constraints. Considering an error tolerance of 0.5 %, the computational time is lower than 1200 s in all cases. For example, the minimum overall cost of the objective function in a PC with an INTEL CORE i7 processor and 16 gigabytes of RAM is obtained in 1040 s after 456,962 iterations, whereas the minimum environmental optimum is reached after 58 s and 7432 iterations.

In spite of using representative days, the size of the problem under study can be bigger than the limits established by commercial solvers for the number of variables and constraints. As advantage, OpenSolver allows solving large-size MILP models without limiting the number of variables and constraints.

In contrast, in the proposed MILP model, non-linear functions that characterize the optimization problem of thermal systems have to be modeled and linearized. Some commercial solvers can automatically linearize a number of nonlinear relationships, but in the case of the OpenSolver, this linearization has to be developed by the engineers or software users. As a contribution to the linear modeling of thermal systems, linear models of the behavior of different generation technologies, thermal storage systems and start-up periods are carried out.

Finally, the interest of proposed model lies in its application in the design or project phase to determine the viability of thermal installations. In this phase, the information provided by the MILP model can be useful to determine the optimal design, sizing and operation mode of heating and DHW installations in any residential building, taking into account the data required for ensuring its feasibility. When the operation of thermal plants has to be optimized, this model can provide qualitative information about the optimal operation mode of the plant. Nevertheless, in the operation strategy optimization of existing plants, metaheuristic methods with non-linear models can adjust better than linear ones and obtain results closer to real operation.

4. Conclusions

This article presents a simple and reproducible MILP-based model for optimizing the configuration, sizing and operation of hybrid systems in residential buildings under economic, environmental and multi-criteria perspectives. This information is essential in the project phase, when the design, sizing and operation of the plant have to be well-defined and the technical feasibility and profitability have to be ensured.

For that, a superstructure is proposed, which includes different thermal generation technologies currently found in the market, as well as photovoltaic modules for electricity production. Thermal generation is divided into two temperature levels in order to consider the possibility of space heating at high or low temperatures. This model is written in a generic way and then, is applied to the building under study. As aforementioned, the proposed model is flexible and can be easily modified and adapted to any residential building and to different technologies.

Regarding the results of the case study, the optimal economic configuration consists of natural gas or electricity fuelled technologies. The DHW is generated by ICE-based micro-CHP and a condensing boiler operating at high temperature; whereas the space heating demand is supplied at low temperature by means of an air-source heat pump and a low temperature boiler. This is largely due to the lower investment cost of these technologies compared to renewable ones and to the high efficiency of cogeneration systems and heat pumps. It should be pointed out that, compared to renewable technologies such as solar thermal or biomass, micro-CHP is considered the most profitable technology for supplying the required minimum contribution to DHW. On the contrary, the optimal environmental structure consists mainly of renewable technologies, such as a biomass boiler, to supply both heating and DHW, with photovoltaic panels for electricity generation. As proven, the economic and environmental criteria are conflicting objectives; so a multi-criteria optimization has been carried out, obtaining an intermediate configuration that encompasses both economic and environmental criteria.

The model is validated by comparing the optimal configurations to the current installation, which has been projected under the same technical, economic and legal conditions. Both the multi-criteria and economic optimums present better economic results than the current plant, while better environmental results are achieved in all optimized cases. Thus, the overall cost decreases by 15% and 8% in the economic and multi-criteria optimal configurations, respectively. Furthermore, the GHG emissions are reduced by 56% and 40% in the environmental and multi-criteria optimal configurations, respectively. According to these results, it can be concluded that the proposed simple and flexible method is efficient for determining the configuration and sizing of thermal hybrid systems of residential buildings in the project phase.

Although the proposed method is applied to a case study, it can be used for determining the optimal installation of any residential building, whatever its technical characteristics and location. Moreover, it has been developed in the Open Source CBC solver, which is implemented in Excel VBA. Thus, the model can be easily implemented and used by engineers and researchers to determine the technical, economic and environmental feasibility of the thermal installations.

Finally, once the optimal configuration is obtained, it would be necessary to carry out a post-optimal study, which would include a more detailed optimization for sizing —not considering the data of generic technologies, but of commercially available products—, as well as the simulation of the operation of the designed plant to optimize the control strategy with metaheuristic methods. This last analysis is beyond the scope of this work.

CRediT authorship contribution statement

E. Pérez-Iribarren: Conceptualization, Methodology, Software, Formal analysis, Validation, Writing – original draft, Writing – review & editing. **I. González-Pino:** Software, Data curation, Formal analysis, Validation, Writing – original draft, Writing – review & editing. **Z. Azkorra-Larrinaga:** Visualization, Investigation, Resources. **M. Odriozola-Maritorena:** Formal analysis, Validation. **I. Gómez-Arriarán:** Visualization, Investigation, Resources.

Declaration of Competing Interest

The authors declare that they have no known competing financial interests or personal relationships that could have appeared to influence the work reported in this paper.

Data availability

Data will be made available on request.

Acknowledgements

This work was supported by the Spanish Ministry of Science and Innovation and the European Regional Development Fund through the SMARTECH project 'Towards Smart Buildings, research of energy monitoring techniques for the evaluation, certification and optimization of control', project reference: PID2021-126739OB-C22 (MCI/AEI/FEDER, UE).

Appendix A. Technical data of building

The building, which is located in Vitoria-Gasteiz (Northern Spain), includes 176 social dwellings and is made up of 10 floors above ground, with 22 dwellings per floor from the 2nd to the 9th floors and storerooms in the floor below the roof. The building comprises 16 different housing models, whose characteristics are summarized in Table A1.

In Table A2 the dwelling models are grouped in thermal zones.

The distribution of thermal zones is shown in the floor plan of the building in Fig. A1.

In Fig. A2 the plan of the south façade in which the photovoltaic panels are placed is shown..

A.1. Thermal and electricity demands

In this section, the operating conditions assumed for the simulation of the building are presented, such as heating setpoint temperatures, ventilation rates and air infiltrations, internal gains and hourly distribution of electricity and DHW demands.

For calculating the heating demand, the thermal transmittances (U-value) of the different enclosures and partitions used in the building are required. These are summarized in Table A.3.

Regarding the windows, its thermal transmittance is 1.1 W/m^2K and its solar factor is 0.40. The frames have a thermal transmittance of 2.2 $W/(m^2 \cdot K)$ and the ratio between the frame surface and the area of the whole window is 26%..

For residential buildings, the schedule of heating setpoint temperatures are defined in [66] with one-hour interval: from 0 a.m to 7 a.m: 17 °C; from 7 a.m to 11p.m: 20 °C; from 11p.m to 12p.m: 17 °C. Besides that, the Spanish Technical Code establishes the ventilation and sanitation requirements in new buildings [67]. These values are shown in Table A4.

With regards to internal gains, these are divided into solar, equipment, lighting and radiative and convective occupancy heat gains. The schedule of these gains, with the exception of solar ones, are summarized in Fig. A.3 and Fig. A.4 for working days and holidays, respectively.

For the calculation of DHW demand, the hourly distribution of DHW consumption is required. As aforementioned in Section 4, the hourly consumption is obtained from the hourly and monthly multiplier factors, which are provided by the Institute for Energy Diversification and Saving (IDAE) [43]. These profiles are shown in Fig. A.5 and Fig. A.6.

In the case of the electricity demand, Spanish Electricity Grid provides the annual and two daily profiles (winter and summer), which are shown in Fig. A.7 and Fig. A.8 [44].

References

[1] Eurostat. An overview (1990-2018); 2020. Available online: < https://ec.europa.eu/eurostat/statistics-explained/index.php/Energy_statistics_-_an_overview >.

[2] Eurostat. Greenhose gas emission statistics - air emissions accounts (2018); 2020. Available online: < https://ec.europa.eu/eurostat/statistics-explained/index.php/Greenhouse_gas_emission_statistics_-_air_emissions_accounts >.
[3] Bloess A, Schill W, Zerrahn A. Power-to-heat for renewable energy integration: A review of technologies, modeling approaches, and flexibility potentials. Appl Energy 2018;212:1611–26.
[4] Wu D, Han Z, Liu Z, Zhang H. Study on configuration optimization and economic feasibility analysis for combined cooling, heating and power system. Energy Convers Manage 2019;190:91–104.
[5] Wang J, Shuwei Li G, Zhang YY. Performance investigation of a solar-assisted hybrid combined cooling, heating and power system based on energy, exergy, exergo-economic and exergo-environmental analyses. Energy Convers. Manage 2019;196:227–41.
[6] Li T, Shahidehpour M. Price-based unit commitment: a case of Lagrangian relaxation versus mixed integer programming. Power Systems, IEEE Transactions on 2005;20:2015–25.
[7] Wang J, Wang J, Yang X, Xie K, Wang D. S A novel emergy-based optimization model of a building cooling, heating and power system. Energy Convers Manage 2022;268:115987.
[8] Aslam S, Khalid A, Javaid N. Towards efficient energy management in smart grids considering microgrids with day-ahead energy forecasting. Electr Power Syst Res 2020;182:106232.
[9] Moser A, Muschick D, Gölles M, Nageler P, Schranzhofer H, Mach T, et al. A MILP-based modular energy management system for urban multi-energy systems: Performance and sensitivity analysis. Appl Energy 2020;261:114342.
[10] Samsatli S, Samsatli NJ. A general mixed integer linear programming model for the design and operation of integrated urban energy systems. J Clean Prod 2018;191:458–79.
[11] Wang X, Jin M, Feng W, Shu G, Tian H, Liang Y. Cascade energy optimization for waste heat recovery in distributed energy systems. Appl Energy 2018;230:679–95.
[12] Carvalho M, Lozano MA, Serra LM. Multicriteria synthesis of trigeneration systems considering economic and environmental aspects. Appl Energy 2012;91:245–54.
[13] Di Somma M, Yan B, Bianco N, Luh PB, Graditi G, Mongibello L, et al. Multi-objective operation optimization of a Distributed Energy System for a large-scale utility customer. Appl Therm Eng 2016;101:752–61.
[14] Di Somma M, Yan B, Bianco N, Graditi G, Luh PB, Mongibello L, et al. Multi-objective design optimization of distributed energy systems through cost and exergy assessments. Appl Energy 2017;204:1299–316.
[15] Dorotić H, Pukšec T, Duić N. Economical, environmental and exergetic multi-objective optimization of district heating systems on hourly level for a whole year. Appl Energy 2019;251:113394.
[16] Mavrotas G, Diakoulaki D, Florios K, Georgiou P. A mathematical programming framework for energy planning in services' sector buildings under uncertainty in load demand: The case of a hospital in Athens. Energy Policy 2008;36:2415–29.
[17] Fazlollahi S, Mandel P, Becker G, Maréchal F. Methods for multi-objective investment and operating optimization of complex energy systems. Energy 2012;45:12–22.
[18] Alarcon-Rodriguez A, Ault G, Galloway S. Multi-objective planning of distributed energy resources: A review of the state-of-the-art. Renew Sustain Energy Rev 2010;14:1353–66.
[19] Iturriaga E, Aldasoro U, Campos-Celador A, Sala JM. A general model for the optimization of energy supply systems of buildings. Energy 2017;138:954–66.
[20] Iturriaga E, Aldasoro U, Terés-Zubiaga J, Campos-Celador A. Optimal renovation of buildings towards the nearly Zero Energy Building standard. Energy 2018;160:1101–14.
[21] Schütz T, Schiffer L, Harb H, Fuchs M, Müller D. Optimal design of energy conversion units and envelopes for residential building retrofits using a comprehensive MILP model. Appl Energy 2017;185:1–15.
[22] Chircop K, Zammit-Mangion D. On-constraint based methods for the generation of Pareto frontiers. J of Mechanics Engineering and Automation 2013;3:279–89.
[23] Campos-Celador Á, Pérez-Iribarren E, Sala JM, del Portillo-Valdés LA. Thermoeconomic analysis of a micro-CHP installation in a tertiary sector building through dynamic simulation. Energy 2012;45:228–36.
[24] Zhu Q, Luo X, Zhang B, Chen Y. Mathematical modelling and optimization of a large-scale combined cooling, heat, and power system that incorporates unit changeover and time-of-use electricity price. Energy Convers Manage 2017;133:385–98.
[25] Moradi S, Ghaffarpour R, Mohammad Ranjbar A, Mozaffari B. Optimal integrated sizing and planning of hubs with midsize/large CHP units considering reliability of supply. Energy Convers. Manage 2017;148:974–92.
[26] Lozano MA, Ramos JC, Serra LM. Cost optimization of the design of CHCP (combined heat, cooling and power) systems under legal constraints. Energy 2010;35:794–805.
[27] Yoshida S, Ito K, Yokoyama R. Sensitivity analysis in structure optimization of energy supply systems for a hospital. Energy Convers Manage 2007;48:2836–43.
[28] Ortiga J, Bruno JC, Coronas A. Selection of typical days for the characterisation of energy demand in cogeneration and trigeneration optimisation models for buildings. Energy Convers Manage 2011;52:1934–42.
[29] Amara F, Agbossou K, Cardenas A, Dubé Y, Kelouwani S. Comparison and simulation of building thermal models for effective energy management. Smart Grid and renew energy 2015;6:95.
[30] Ministry of Health and Consumption. Royal Decree 865/2003, of 4 July, establishing the hygienic criteria for the prevention and control of legionellosis; 2003 [in Spanish].
[31] Sech Project-Spahousec. Analyses of the energy consumption of the household sector in Spain, Final Report; 2011.
[32] Pérez-Iribarren E, González-Pino I, Azkorra-Larrinaga Z, Gómez-Arriarán I. Optimal design and operation of thermal energy storage systems in micro-cogeneration plants. Appl Energy 2020;265:114769.
[33] González-Pino I, Pérez-Iribarren E, Campos-Celador A, Terés-Zubiaga J. Analysis of the integration of micro-cogeneration units in space heating and domestic hot water plants. Energy 2020;200:117584.
[34] Mason AJ, Dunning I. OpenSolver: Open Source Optimisation for Excel. Proceedings of the 45th Annual Conference of the ORSNZ (Operations Research Society of New Zealand). 2010.
[35] Winston WL, Goldberg JB. Operations research: applications and algorithms. Duxbury press Boston; 2004.
[36] Soleimani-damaneh M. Modified big-M method to recognize the infeasibility of linear programming models. Knowl-Based Syst 2008;21:377–82.
[37] Carvalho M. Thermoeconomic and environmental analyses for the synthesis of polygeneration systems in the residential-commercial sector. PhDThesis 2011.
[38] Wärmepumpen-Testzentrum WPZ Buchs. Test results air/water heat pumps based on the EN 14511, WPZ-Bulletin N.01; 2010 [in German].
[39] Directive 2012/27/EU of the European Parliament and of the Council of 25 October 2012 on energy efficiency, amending Directives 2009/125/EC and 2010/30/EU and repealing Directives 2004/8/EC and 2006/32. Official Journal. 2012;315: 1-56.
[40] Ministry of Industry, Energy and Tourism. Royal Decree 413/2014, of June 6th, on the regulation of the electricity production activity based on renewable energies, cogeneration and wastes (BOE n.140); 2014 [in Spanish].
[41] E. Pérez-Iribarren. Operation and design optimization of microcogeneration plants for residential buildings; 2016 [in Spanish].
[42] CTE (Spanish Technical Building Code). Basic Document HE 4: Solar Minimum Contribution for Domestic Hot Water. Ministry of Housing, Spanish Government; 2013 [in Spanish].
[43] IDAE (Institute for Energy Diversification and Saving). Evaluation of the potential of solar thermal air conditioning in buildings. Institute for Energy Diversification and Saving, Ministry of Industry, Tourism and Commerce, Spanish Government; 2011 [in Spanish].
[44] REE, Spanish electricity grid (in Spanish). Available online: <www.ree.es>.
[45] EVE (Basque Goverment Energy Agency). Energy keys to domestic sector in the Basque Country; 2013 [in Spanish].
[46] Atecyr (Spanish Technical Association of HVAC). Technical Guideline DTIE 18.03: Integration of Renewable Energies on Energy Rehabilitation in Buildings; 2013 [in Spanish].
[47] Cockroft J, Samuel A, Tuohy P. Development of a Methodology for the Evaluation of Domestic Heating Controls. Phase 2 of a DEFRA Market Transformation Programme project, carried out under contract to BRE Environment. Final Report 2007.
[48] AVEBIOM (Spanish Association for Energy Recovery from Biomass). Recognized document: New performance correction curve with par-load factor for biomass boilers; 2011 [in Spanish].
[49] ASUE (A. für Sparsamen, U. Energieverbrauch Ev). CHP characteristics 2011: modules, providers, costs. Publishing house for economical and environmentally friendly energy consumption; 2011 [in German].
[50] L. Jutglar, A.L. Miranda, M. Villarrubia. FERROLI Heating manual; 2011 [in Spanish].
[51] Meteotest. Meteonorm Global Meteorological Database, Version 7; 2017.
[52] Ertesvåg IS. Uncertainties in heat-pump coefficient of performance (COP) and exergy efficiency based on standardized testing. Energy Build 2011;43:1937–46.
[53] IDAE, Technical Guide N°3. Design and calculation of the thermal insulation of pipes, appliances and equipment. Institute for Energy Diversification and Saving, Ministry of Industry, Tourism and Commerce, Spanish Government; 2007 [in Spanish].
[54] Construction Technology Institute ITeC. BEDEC Database; 2019. Available online: <https://metabase.itec.cat/vide/es/bedec >.
[55] CYPE Ingenieros. Software for Architecture, Engineering and Construction, Price Generator Database; 2019. Available online: < http://www.generadordeprecios.info/ >.
[56] IDAE (Institute for Energy Diversification and Saving). Eligibility guide of projects in charge of the JESSICA F.I.D.A.E holding fund. Institute for Energy Diversification and Saving, Ministry of Industry, Energy and Tourism, Spanish Government; 2014 [in Spanish].
[57] European Union Regional Policy. Guide to cost benefit analysis of investment projects; 2008. Available online: < https://ec.europa.eu/regional_policy/sources/docgener/studies/pdf/cba_guide.pdf >.
[58] Ministry of Industry, Energy and Tourism. Order IET/1045/2014, of June 16th, on the approval of the retributive parameters of the reference installations applicable to certain electricity production plants based on renewable energies, cogeneration and wastes (BOE n.150); 2014 [in Spanish].
[59] Wernet G, Bauer C, Steubing B, Reinhard J, Moreno-Ruiz E, Weidema B. The ecoinvent database version 3 (part I): overview and methodology. Int J Life Cycle Assess 2016;21:1218–30.
[60] IDAE (Institute for Energy Diversification and Saving). CO2 emission factors and primary energy coefficients of different end-use energy consumptions in the building sector in Spain. Ministry of Industry, Tourism and Commerce; 2016 [in Spanish].
[61] IDAE (Institute for Energy Diversification and Saving). Solar Thermal Energy Installations, Technical Specifications for Low Temperature Installations, PET-REV; 2009 [in Spanish].
[62] ASIT (Solar Thermal Industry Association). ASIT Solar design guide; 2010 [in Spanish].

[63] Commission Decision 2007/74/EC. Commission Decision of 21 December 2006 establishing harmonised efficiency reference values for separate production of electricity and heat in application of Directive 2004/8/EC of the European Parliament and of the Council; 2007.
[64] Ministry of Industry, Tourism and Commerce. Royal Decree 661/2007, of May 11th, on the promotion of cogeneration (BOE n.114); 2007 [in Spanish].
[65] Ministry of Industry, Energy and Tourism. Resolution of January 31st of the General Administration on Energy Policy and Mines, on the publication of the production of electric energy and the voluntary prices for small consumers (BOE n.28); 2014 [in Spanish].
[66] IDAE (Institute for Energy Diversification and Saving). Conditions for the acceptance of alternative software. Annexes. Ministry of Industry, Tourism and Commerce; 2009 [in Spanish].
[67] CTE (Spanish Technical Building Code). Basic Document HS 3: Health Standars, Spanish Government; 2013 [in Spanish].